Macroscopic Carbon Nanotube-based 3D Monoliths

*Ran Du, Qiuchen Zhao, Na Zhang, and Jin Zhang**

From the Contents

Carbon nanotubes (CNTs) are one of the most promising carbon allotropes with incredible diverse physicochemical properties, thereby enjoying continuous worldwide attention since their discovery about two decades ago. From the point of view of practical applications, assembling individual CNTs into macroscopic functional and high-performance materials is of paramount importance. For example, multiscaled CNT-based assemblies including 1D fibers, 2D films, and 3D monoliths have been developed. Among all of these, monolithic 3D CNT architectures with porous structures have attracted increasing interest in the last few years. In this form, theoretically all individual CNTs are well connected and fully expose their surfaces. These 3D architectures have huge specific surface areas, hierarchical pores, and interconnected conductive networks, resulting in enhanced mass/electron transport and countless accessible active sites for diverse applications (e.g. catalysis, capacitors, and sorption). More importantly, the monolithic form of 3D CNT assemblies can impart additional application potentials to materials, such as free-standing electrodes, sensors, and recyclable sorbents. However, scaling the properties of individual CNTs to 3D assemblies, improving use of the diverse, structure-dependent properties of CNTs, and increasing the performance-to-cost ratio are great unsolved challenges for their real commercialization. This review aims to provide a comprehensive introduction of this young and energetic field, i.e., CNT-based 3D monoliths, with a focus on the preparation principles, current synthetic methods, and typical applications. Opportunities and challenges in this field are also presented.

1. Introduction

Carbon nanotubes (CNTs), one of the most promising carbon allotropes with a tubular geometry constructed from sp^2 carbon atoms, have drawn tremendous attention since their discovery over two decades ago.[1–8] Thanks to their nanoscale size and special arrangement of carbon atoms, CNTs display superior physicochemical properties (e.g. mechanical, electrical, and optical) and thus possess great potential for diverse applications. The application fields can be roughly divided into two classes: microscopic electronic devices (e.g. field-effect transistors, chemical sensors, field emitters, and nano-tweezers),[9–13] and macroscopic applications (e.g. structural materials, conductors, electrode materials, and composites).[14–21] Because of the wide application scope and simplicity toward industrialization, tremendous efforts have been made in the latter direction. Consequently, multiscaled CNT-based macroscopic assemblies, including 1D CNT fibers/yarns, 2D CNT films/sheets/horizontally aligned arrays, and 3D CNT gels/sponges/vertically aligned CNT (VA-CNT) arrays have been rapidly developed.[15]

In the past few years, the perception of CNTs' structures and properties has been greatly improved, and CNT-based macroscopic assemblies have penetrated many fields and created considerable benefits (see **Figure 1**).[4–7,14] However, the key problem—scaling the properties of individual CNTs (e.g. high specific surface area (SSA), mechanical strength, and electrical conductivity) to a macroscopic level—is still unsolved.[6] The lack of scalability can greatly impact the exceptional properties of CNTs, thereby lowing their performance-to-cost ratio. For example, the strength of most reported CNT fibers is less than 10 GPa, significantly lower than that of individual CNTs (up to 100 GPa).[6,15] Two reasons may account for this issue: the structure–property relationships of CNT-based assemblies have not been well understood because of the astonishing complexity of macroscopic assemblies, and the efficient preparation strategies to realize precise structural control are lacking.

One promising way to address the above problems is to assemble CNTs into 3D porous monoliths, such as aerogels, foams, and sponges (for simplicity, all of them are called aerogels in this manuscript). Aerogels are a kind of free-standing 3D assembly with open and hierarchical pores, interconnected networks, huge SSAs, and a monolithic form.[22–24] Aerogels based on silica, carbon, metal oxides, and metals have been fabricated and studied extensively for years,[25–28] but aerogels based on CNTs are a new form. The unique structure of the aerogel facilitates the exposure and connection of nearly all CNTs, thus providing enormous opportunities for releasing the potential of CNTs and creating high-performance materials.

As a rising star in both aerogel and CNT fields, the opportunities and challenges of the CNT-based aerogels coexist. Firstly, compared with their 2D analogues (graphene), the 1D geometry of CNTs places a great barrier in front of the preparation of monolithic assemblies because of their less effective inter-tube π–π interactions.[29] Hence the development of efficient preparation techniques is highly desired. On the other hand, due to the tubular geometry and less effective inter-tube π–π interactions, CNT-based aerogels are expected to present a larger surface area than their graphene-based analogues. Secondly, CNTs not only show incredible physicochemical properties (e.g., mechanical, electrical, thermal, and optical), but also exhibit huge diversities in the number of walls, diameters, lengths, junctions, and chirality. These diversities have a great effect on the properties of CNT assemblies and can provide CNTs with rich application potential. For instance, the specific surface area of CNTs (also for CNT assemblies) correlates negatively to the number of walls present, thus, few-walled CNTs or even single-walled CNTs (SWCNTs) are preferable for catalysis and gas sorption because of their large number of active sites. For another example, electrical properties of CNTs are directly determined by their chirality. Hence, for conductors and electrochemical catalysis, all-metallic CNTs would be a better choice. However, although a recent extraordinary work presented by Yang and co-workers showed the possibility to realize good control of these parameters,[30] their precise control is still a great challenge. In addition, the structure–property relationships of CNT-based 3D monoliths have not been established. Finally, from the standpoint of practical applications, great endeavors are required to scale the performance of individual CNTs to macroscopic CNT-based aerogels and lower the cost of fabrication methods (including for pristine CNTs and aerogels). Currently, the performance-to-cost ratio of CNT-based aerogels in many applications (e.g., energy storage, electrochemical catalysis, or water treatment) cannot compete with other materials such as graphene-based aerogels, carbon aerogels, and carbon-fiber aerogels. The development of CNT-based 3D aerogels is still in its infancy.

Herein we aim to provide a comprehensive picture and state-of-the-art review of the CNT-based 3D monoliths, with a focus on the design principles, synthetic methods, and potential applications. In this context, the concept of 3D monoliths will be very restricted. The third dimension must be be comparable to the other two dimensions, and all three dimensions must be macroscopic. Secondly, materials should be free-standing, highly porous monoliths. Hence, the term "monoliths" is equal to "aerogels" in this context. Since most CNT-based aerogels are derived from wet gels, the preparation principles of CNT-based wet gels will also be introduced.

In the first section, the structure, properties, and related macroscopic assemblies of CNTs are briefly introduced. The second section focuses on the synthetic principles and strategies towards CNT-based 3D monoliths. After a summary

R. Du, Q. C. Zhao, N. Zhang, Prof. J. Zhang
Center for Nanochemistry, Beijing National Laboratory for Molecular Sciences
Key Laboratory for the Physics and Chemistry of Nanodevices
State Key Laboratory for Structural Chemistry of Unstable and Stable Species
College of Chemistry and Molecular Engineering
Peking University
Beijing 100871, PR China
E-mail: jinzhang@pku.edu.cn

DOI: 10.1002/smll.201403170

small NANO MICRO

of the typical characterization methods and applications of those materials, some perspectives on the future opportunities of CNT-based 3D monoliths conclude this review.

2. Structures, Properties and Macroscopic Assemblies of CNTs

Both experiments and theoretical calculations suggest that individual CNTs have exceptional physicochemical properties (e.g., mechanical, electrical, thermal, and optical).[3,7] Therefore, CNTs have continuously drawn worldwide attention in multiple disciplines including chemistry, physics, biology, and materials science. For making macroscopic functional materials, CNTs are required to be converted into multiscaled macroscopic assemblies such as 1D fibers, 2D sheets, and 3D aerogels. However, great challenges lie in scaling the properties of individual CNTs to a macroscopic level and truly realizing these amazing properties in practical applications.

2.1. Structures and Properties of CNTs

An individual CNT can be visualized as a high-aspect-ratio ($\approx 10^2$–10^8) tube formed by graphene layers seamlessly rolled in a specific direction (**Figure 2**a).[31] According to the number of graphene layers, the CNTs can be divided into single-walled carbon nanotubes (SWCNTs), double-walled carbon nanotubes (DWCNTs), or multi-walled carbon nanotubes (MWCNTs). Regarding the hexagonal symmetry of the graphene layer, the SWCNT will obtain a specific chirality according to the rolling fashion. The chirality is always expressed as a chiral vector (roll-up vector):

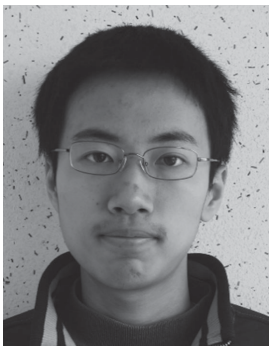

Ran Du received his B.S. from the Beijing Institute of Technology in 2011. He then joined Prof. J. Zhang's group to pursue a PhD in the College of Chemistry and Molecular Engineering, Peking University. His current research interests lie in the synthesis of macroscopic, multifunctional, and porous carbon nanotube-based materials and other porous materials for applications in energy, catalysis, and environmental related fields.

Jin Zhang received his PhD from Lanzhou University in 1997. After a two-year postdoctoral fellowship at the University of Leeds, UK, he joined Peking University where he was appointed Associate Professor (2000) and then promoted to Full Professor in 2006. His research focuses on the controlled synthesis and spectroscopic characterization of carbon nanomaterials.

$$\vec{C} = n\vec{a_1} + m\vec{a_2} \quad (1)$$

where $\vec{a_1}$ and $\vec{a_2}$ represent the two unit vectors along the zig-zag edge, while the pair of integers (n,m), known as the chiral index, are the steps along the zig-zag carbon bonds of corresponding unit vectors. Hence the structure (except for

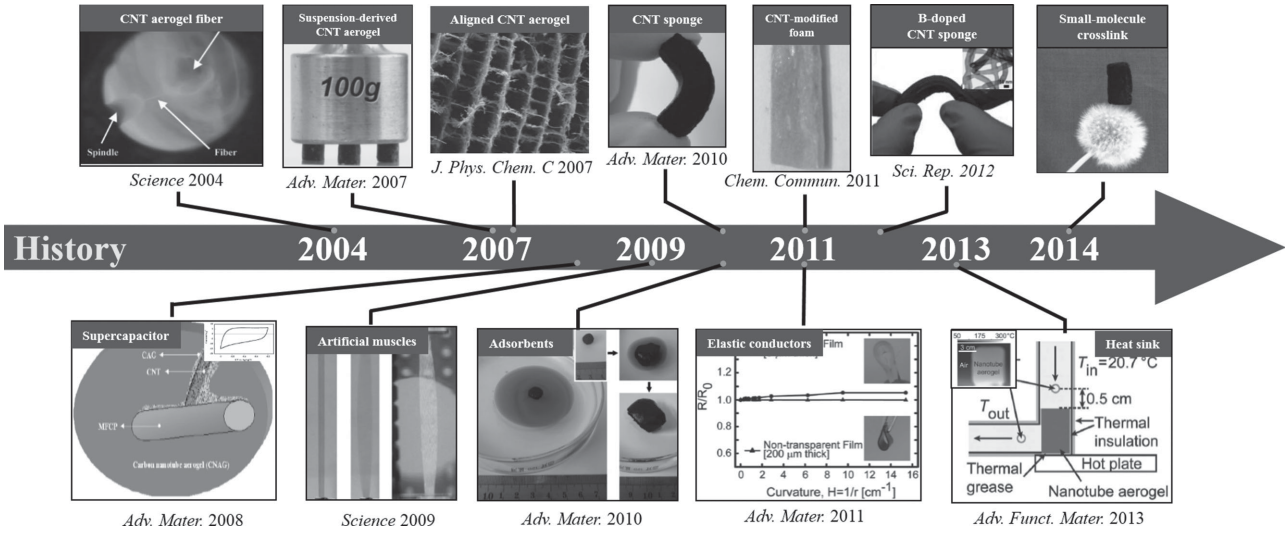

Figure 1. The history of CNT-based aerogels. Top Row (from left): 1st image reproduced with permission.[43] Copyright 2004, American Association for the Advancement of Science; second image reproduced with permission.[53] Copyright 2007, Wiley-VCH; 3rd image reproduced with permission.[127] Copyright 2007, the American Chemical Society; 4th image reproduced with permission.[55] Copyright 2010, Wiley-VCH; 5th image reproduced with permission.[123] Copyright 2011, Royal Society of Chemistry; 6th image reproduced with permission.[65] Copyright 2012, Nature Publishing Group. Bottom Row (from left): 1st image reproduced with permission.[152] Copyright 2009, Wiley-VCH; 2nd image reproduced with permission.[170] Copyright 2005, American Association for the Advancement of Science; 3rd image reproduced with permission.[55] Copyright 2010, Wiley-VCH; 4th image reproduced with permission.[167] Copyright 2008, Wiley-VCH; 5th image reproduced with permission.[106] Copyright 2013, Wiley-VCH.

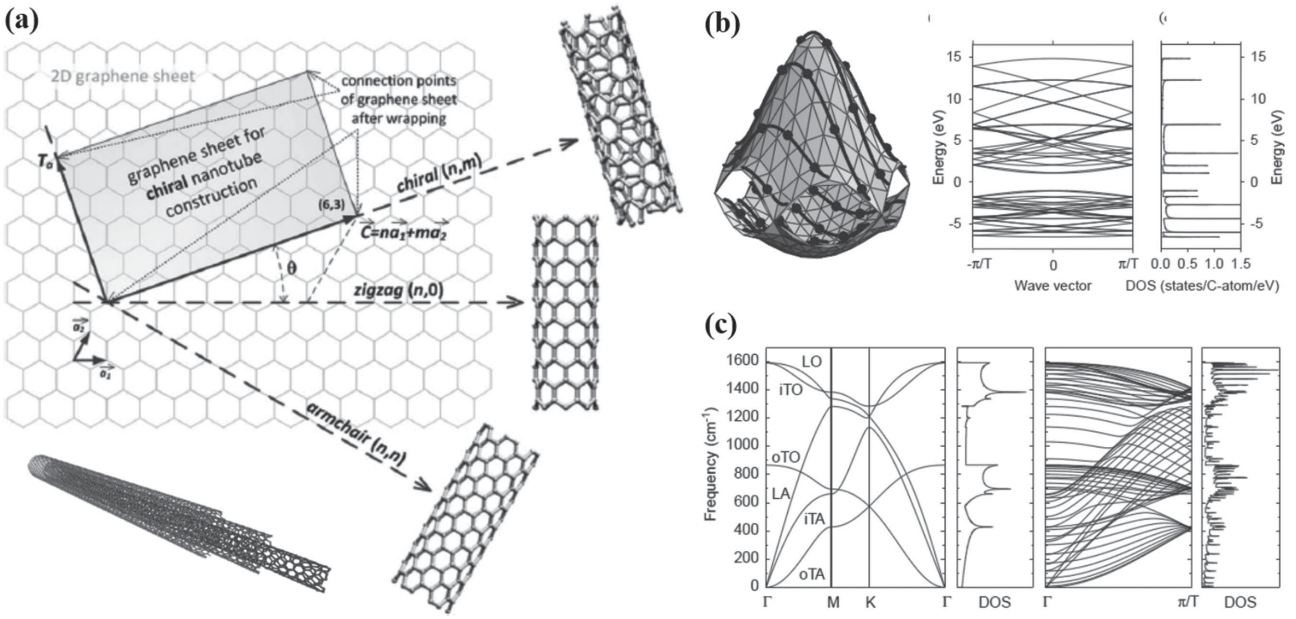

Figure 2. a) The relationship between CNTs and graphene. Reproduced with permission.[31] Copyright 2011, Royal Society of Chemistry. b) The calculated electronic structure of graphene and the cutting line (solid curves) of a (4,2) tube (left), the energy states and density of states (DOS) of a (4,2) tube (middle and right). c) Left are the phonon dispersion relation and corresponding phonon density of states for a 2D graphene sheet. Right are calculated phonon dispersion relation and corresponding phonon DOS of a (10,10) tube. Reproduced with permission.[32] Copyright 2005, Elsevier Publishing Group.

length) of an individual SWCNT (the rolling direction $\vec{C}$ and the diameter $|\vec{C}|$) can be unambiguously determined by a chiral vector. Chirality has large impact on properties of SWCNTs, especially on their electronic structures and phonon dispersion relations (Figure 2b,c).[32] Based on the chiral index (n,m), the electronic properties of SWCNTs can be classified as i) metallic, when $n = m$, ii) semiconducting, with a tiny bandgap when $n–m = 3k$ (k is a non-zero integer), and iii) semiconducting, with a bandgap inversely depending on the tube diameter (all other SWCNTs). For perfect MWCNTs, the electronic properties are similar to SWCNTs because of weak coupling between cylinders in MWCNTs.[4] Therefore, CNTs show a greater structure and property diversity, overwhelming their 2D analogue graphene at the nanoscale level. Both the challenges and opportunities regarding the use of CNTs involve this diversity.

In addition to their structure-dependent diversity, individual CNTs also display many other incredible properties. For example, their excellent mechanical properties (elastic moduli up to 1 TPa and tensile strengths up to 250 GPa) and high thermal stability (up to 650 °C in an oxidizing atmosphere and 2800 °C in vacuum) make them useful in harsh conditions or for structure-supporting materials.[3,7] Fully conjugated backbones impart an ultrahigh electrical current-carrying capacity (up to 1000 times higher than that of copper) and thermal conductivity (6000 W m^{-1} K^{-1}, nearly double that of diamond).[7] The high SSA, especially for SWCNTs (theoretically 1315 m^2 g^{-1}), affords great potential for catalysis, adsorption, and many energy-related fields. The unique hollow-tube geometry with a diameter ca. 1–100 nm may provide a special environment for studying space-limited reactions.

CNTs can be prepared by arc discharge, laser ablation, chemical vapor deposition, and hydrothermal methods, etc., which have been well reviewed by Prasek and co-workers and Chen and co-workers.[31,33] Purification is another important subject, since as-prepared CNTs always contain carbonaceous and metallic impurities which may affect their intrinsic properties. The purification methods can be classified as chemical oxidation methods (e.g., gas-phase oxidation, liquid-phase oxidation, electrochemical oxidation), physical-based methods (e.g., filtration, centrifugation, annealing), or multi-step methods (e.g., sonication in combination with oxidation). The details of purification techniques, evaluation methods, and possible effects of the purity on CNT properties have been well studied and are reviewed elsewhere.[34–36]

2.2. CNT-based Macroscopic Assemblies

Since most practical applications require macroscopic materials, it is necessary to integrate individual CNTs into macro-level assemblies while maintaining their remarkable properties. In the last two decades, 1D, 2D, and 3D CNT-based assemblies with either CNT composites or exclusive CNTs have been extensively studied (**Figure 3**). The preparation methods can be roughly classified to two classes, i.e., dry chemistry (chemical vapor deposition growth, spinning from VA-CNT arrays or aerogels) and wet chemistry (from CNT-based dispersions). The former method always creates high-quality materials made up of long individual CNTs, while the later approach possesses much more flexibility due to a decoupling of the CNT growth and assembly steps. Comprehensive reviews of macroscopic assemblies of CNTs are

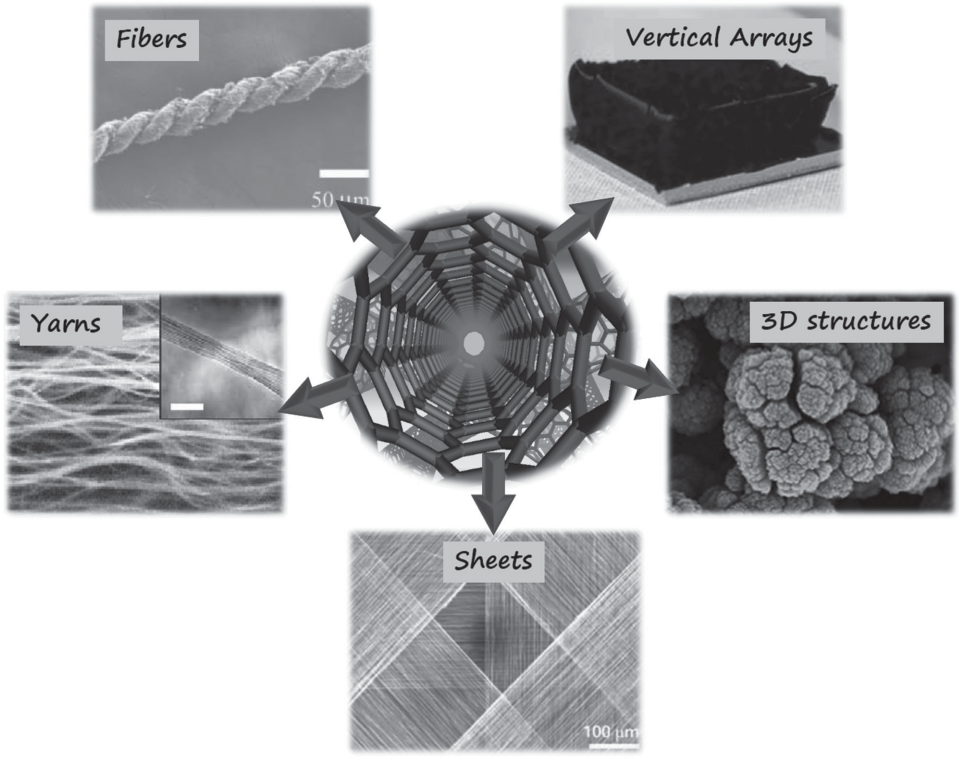

Figure 3. The different macroscopic assemblies of CNTs. 'Fibers' reproduced with permission.[43] Copyright 2004, American Association for the Advancement of Science; 'Vertical Arrays' reproduced with permission.[62] Copyright 2004, American Association for the Advancement of Science; 'Yarns' reproduced with permission.[42] Copyright 2002, Nature Publishing Group; '3D Structures' reproduced with permission.[56] Copyright 2012, Royal Society of Chemistry; 'Sheets' reproduced with permission.[47] Copyright 2005, American Association for the Advancement of Science.

given by Zhang and co-workers[15] and Chan-Park and co-workers.[37] In this section, we just give a brief introduction to various CNT-based assemblies, according to their dimensions.

2.2.1. One-Dimensional CNT-based Assemblies

Controlled orientation is very useful to enhance the performance of materials in a specific direction. 1D fibers are one of the typical aligned aggregation states which have been widely adopted in the polymer industry. Similarly, 1D CNT-based assemblies (fibers or yarns) are derived from spinning CNTs into aligned fibers along the spinning direction, thereby maximizing the axial properties of materials. CNT fibers are acquired from either liquid (surfactant-based dispersions[38] or super-acid-based dispersions[39–41] or solid-state (VA-CNT arrays[42] or by growing CNT aerogels in a chemical vapor deposition system[43,44] spinning. Thanks to the unique features of CNTs, the resultant fibers not only enjoy a high Young's modulus (up to hundreds of gigapascals), comparable to commercial polymer fibers such as Kevlar fibers, but also exhibit excellent electrical conductivities (up to 5000 S cm^{-1}). A comprehensive introduction to CNT fibers is provided elsewhere.[45,46]

2.2.2. Two-Dimensional CNT-based Assemblies

2D CNT-based films and sheets have also received considerable attention because of their remarkable electrical and thermal conductivity, high flexibility, and high stability. They have therefore found wide application, ranging from transparent conductive films, separators, polarized light sources, to loudspeakers.[47,48] Similar to CNT fibers, films can also be obtained by either wet methods (e.g., vacuum filtration, Langmuir–Blodgett deposition)[15,49] or dry methods (e.g., drawn from VA-CNT arrays,[50,51] direct chemical vapor deposition growth[52].

2.2.3. Three-Dimensional CNT-based Assemblies

In recent years, CNT-based 3D architectures have received growing interest.[53–57] Among them, low-density and porous monoliths (aerogels) have shown great potential for wide application. The aerogels are a kind of monolithic, 3D, solid network containing interconnected pores. This guarantees their high porosity, low density, and huge specific surface area, thus facilitating their wide application scope such as for scaffold materials, electrode materials, and catalysis.[23,24,27] The appearance of new materials, e.g., CNTs, has greatly accelerated the development of aerogels. Combining the features of aerogels (hierarchical pores, low density, high SSA, and high porosity) and remarkable properties of CNTs (high conductivity, high strength, high surface area, and low atomic weight), CNT-based aerogels can not only realize the exceptional potential of CNTs, but may also impart some new functionality to aerogels.

The concept of CNT aerogels first appeared in 2004,[43] where the CNT fibers were spun from the CNT aerogels in a chemical vapor deposition (CVD) system. After a three-year

silence, the research was revisited by Bryning and co-workers, who created highly conductive few-walled CNT (FWCNT) aerogels from a CNT suspension.[53] Another encouraging breakthrough was made by Gui and co-workers in 2010, where the CVD technique was established for growing isotropic CNT sponges.[55] Following these pioneering works, CNT-based aerogels have received wide attention, and both their fundamental properties and practical applications have been extensively studied (see Figure 1). However, due to the lack of efficient methods to finely modulate the microstructures of these materials and to control the type of CNT produced (e.g., number of walls, chirality, doping), the true potential of CNT aerogels has still not been realized. Combined with the high cost of CNT precursors, the low performance-to-cost ratio of CNT-based aerogels has made them less competitive with other materials such as graphene-based aerogels and carbon aerogels. Therefore, there is large room for improvement in this young field.

3. Synthetic Strategies for CNT-based Monoliths

To acquire a 3D porous network, either dry chemistry methods (direct growth by CVD) or wet chemistry methods (produce the network in the solution and then take out the inside solvent) can be adopted. The former method can produce mechanically flexible and highly conductive CNT aerogels composed of high-quality and long individual CNTs, while the latter approach enjoys tunable composition, well-controlled reaction conditions, easy functionalization and scalability.

However, both of these methods have inherent drawbacks. CVD-grown CNT monoliths always include a considerable amount of metal catalyst which cannot be removed by normal acid purification, affecting studies of the intrinsic properties of CNT aerogels, especially for catalysis. One-step growth also makes it extremely difficult to control the type (e.g., number of walls, chirality) of as-grown CNTs, since in-situ control over the growth of CNTs is still a great hurdle in CNT preparation. The wet chemistry approach requires a good CNT dispersion before reaction. During the dispersing step, CNTs are always cut down to several hundreds of nanometers and many defects can be introduced, resulting from ultrasonication or oxidation, largely deteriorating the properties of pristine CNTs.

Therefore, simultaneous control over the type and functionalization of CNTs in aerogels is far from satisfactory by existing methods, which in turn impairs their superior properties as predicted by theoretical calculations. Fortunately, some modified or brand-new strategies have been injected into this young field. Moreover, the preparation strategies of analogues such as graphene aerogels may also provide many useful hints.[29,58,59] However, at this stage, efficient approaches are still highly desired to realize well-controlled CNT structures in aerogels.

3.1. CNT-based Monoliths Prepared by CVD

Chemical vapor deposition is a frequently used technique for CNT preparation. Generally, the carbon sources are decomposed on the surface of catalyst particles at high temperature, then nanotubes are grown from the nanosized particles according to either vapor–liquid–solid (VLS) or vapor–solid (VS) mechanisms.[8] Therefore, it is natural to come to the idea of directly growing CNT aerogels by the CVD technique (**Figure 4**a). Based on the catalyst's formation and reaction conditions, the CVD method can produce either vertically aligned CNT arrays or isotropic CNT sponges constructed from high-quality and long individual CNTs, important for achieving exceptional electrical and mechanical performance. In contrast, although graphene can also be prepared by the CVD process, the direct growth of free-standing graphene monoliths without a template is impossible. For the CVD fabrication method, two main issues have puzzled scientists: the in-situ control of as-grown CNT types, and the removal of metal impurities without affecting the aerogel qualities.

3.1.1. Ultralong VA-CNT Arrays

Vertically aligned CNT arrays are always fabricated by flowing carbon sources over a substrate sputtered by metal thin film as a catalyst, where the alignment comes from a "crowding effect" between CNTs.[60] Although VA-CNT arrays have been acquired for years,[61] the thickness of the arrays (typically less than 1 mm) are usually much shorter than the other two dimensions. Hence they cannot be regarded as true 3D CNT monoliths. Fortunately, thanks to an increasing understanding of the mechanisms and the role of each parameter (e.g., carbon source concentration, hydrogen concentration, water vapor, substrate design, deposition temperature) for CNT growth, long VA-CNT arrays have been obtained.[57,62,63] For example, Hata's group reported the growth of superdense 2.5 mm-high SWCNT arrays with the assistance of water vapor, where the water was believed to promote growth by eliminating amorphous carbon and thus enhancing the catalyst's life.[62] Recently, Cho and co-workers successfully acquired ultralong VA-CNT arrays with thicknesses up to 2 cm (Figure 4b).[57] In this study, the ethylene/hydrogen ratio and water concentration were carefully investigated. Additionally, they claimed that the introduction of hydrogen not only removed amorphous carbon, but also counteracted oxygen to reduce its etching effect.

It can be envisaged that these anisotropic 3D CNT monoliths would show intriguing properties or enhanced performance in many cases (e.g., anisotropic mechanical properties, enhanced electrical conductivity parallel to the CNT growth direction), but the potential of this field is still underexploited. This may be attributed to two big challenges. For most cases, the growth time is quite long (several to tens of hours) for obtaining a sufficient height, which is very energy- and time-consuming, thus increasing the production cost. In addition, the vertical growth originates from crowding effects of CNTs, which means that CNTs are arranged side by side to support the monolithic structure. In this way, considerable surface areas of individual CNTs may not be accessible because of this close-packing style. In fact, the specific surface area of VA-CNT arrays have hardly been reported in the literature. There are, therefore, countless opportunities

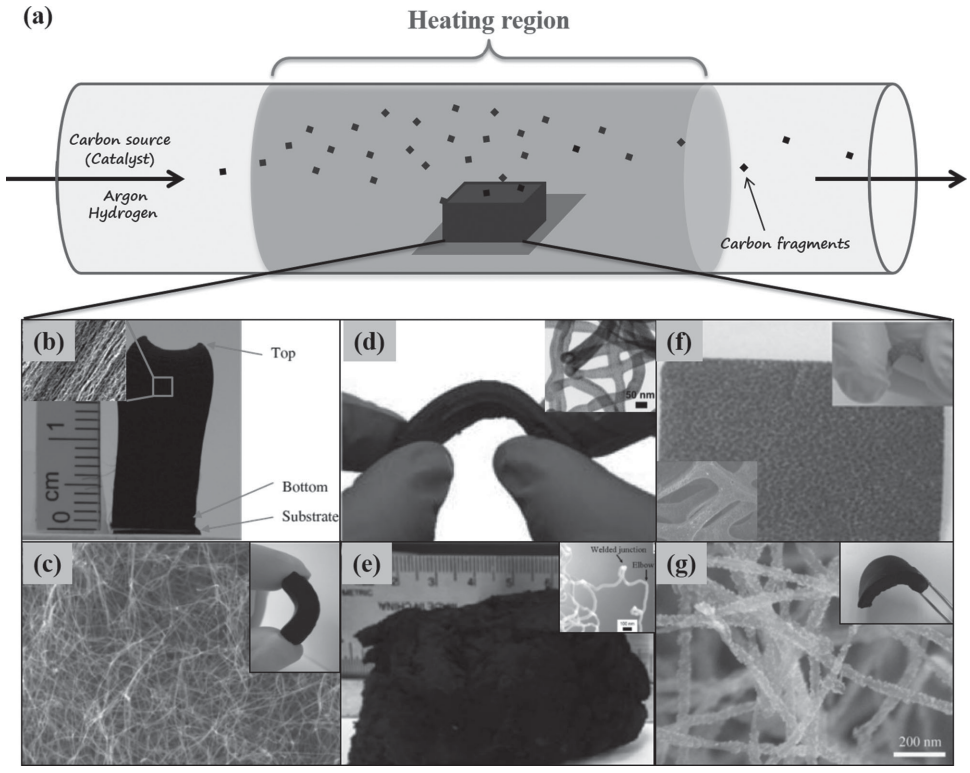

Figure 4. a) The schematic illustration of 3D CNT monoliths prepared by the CVD method, and corresponding examples such as b) ultralong CNT vertical arrays (reproduced with permission.[57] Copyright 2014, Elsevier Publishing Group), c) CNT sponges (reproduced with permission.[55] Copyright 2010, Wiley-VCH), d) boron-doped CNT sponges (reproduced with permission.[65] Copyright 2012,Nature Publishing Group), e) nitrogen-doped CNT sponges (reproduced with permission.[66] Copyright 2013, the American Chemical Society), f) a graphene–CNT hybrid foam (reproduced with permission;[67] copyright 2012, Royal Society of Chemistry), and g) a CNT sponge grafted with CdS nanoparticles (reproduced with permission;[72] copyright 2012, Springer Publishing).

in the field of ultralong VA-CNT arrays for both preparation and application.

3.1.2. Isotropic CNT Monoliths

Aside from aligned ultralong VA-CNT arrays, 3D isotropic CNT monoliths can also be created by the CVD technique. To achieve isotropy, floating catalysts are always used. In 2004, the concept of isotropic CNT aerogels was first introduced by Windle's group.[43] They injected an ethanolic solution of ferrocene and thiophene (ethanol for carbon sources, ferrocene for catalysts, and thiophene for promoters) in the furnace carried by hydrogen gas, and the quick formation of the aerogel was viewed by a mirror. However, the focus of this work is on the CNT fibers spun from the aerogel. Similar to the approach applied to VA-CNT arrays, Zheng and coworkers prepared CNT cotton on a silicon substrate.[64] The difference here was that metal catalysts were just applied to one edge of the substrate. The resultant cotton was constructed by randomly oriented long CNTs, but the thickness was only several millimeters.

In 2010, truly 3D isotropic CNT sponges were synthesized by Gui et al.,[55] where a dichlorobenzene solution of ferrocene taken by the carrier gases (a mixture of argon and hydrogen) was injected into the furnace. After a 4 h growth period, MWCNT sponges with low densities (about 5–10 mg cm^{-3}) were acquired on the pre-inserted quartz sheet substrate (Figure 4c). This pioneering work provides a feasible way to prepare macroscopic isotropic truly 3D CNT sponges in a CVD system, and demonstrates the incredible mechanical and electrical properties of the resultant materials. However, the sponge possessed a low specific surface area (SSA) of only 62.8 m^2 g^{-1}, which may be attributed to the large diameters of the MWCNTs. In fact, the in-situ control of CNT diameters and other parameters (such as chirality) are great challenges for CVD-grown sponges.

Doping heteroatoms into the carbon lattice is expected to endow some intriguing properties to CNTs, such as altered hydrophobicity, enhanced electrical conductivity, and preferred sorption towards specific species (e.g., O_2 sorption for nitrogen-doped CNTs). CVD provides a facile way to realize one-pot growth of 3D heteroatom-doped CNT monoliths. Following the creation of pristine CNT sponges, boron-doped and nitrogen-doped CNT sponges were also obtained (Figure 4d,e) by introducing a heteroatom-containing source (e.g., triethylborane for boron doping, pyridine for nitrogen doping) in the precursor solution.[65,66] In this way, heteroatoms created by the decomposition of precursors at high temperature could be incorporated in situ into the carbon lattice during the growth process (ca. 0.7 at% for boron and 4.28 at% for nitrogen). More interestingly, it was observed

that the heteroatoms could create strong covalent bonding between different CNTs in the form of "elbow" joints, which can serve as springs to enhance the reversible elastic deformation of sponges.[65]

3.1.3. Template-derived CNT-based Monoliths

Sometimes, the preparation of 3D CNT-based monoliths with a porous template (always a metal foam) can be very beneficial. The template can not only tailor the pore-size distribution (PSD) of macro- or mesopores in aerogels, but also suppresses the aggregation of the growing CNTs to some extent. After growth, the template is removed, giving rise to free-standing 3D monoliths.

Dong and co-workers reported a graphene–carbon nanotube hybrid foam via a two-step CVD process (Figure 4f).[67,68] In this approach, graphene flakes were grown on the nickel foam at first, then CNTs were grown on the graphene/nickel foam after Ni particle loading. A one-step preparation approach has also been demonstrated by Wang and co-workers,[69] where an iron catalyst layer was deposited on the nickel foam before conducting ambient pressure CVD (APCVD).

However, currently, nickel foams seem to be almost the only template for CNT-based monolith preparation. Therefore, only CNT/graphene composite monoliths can be created, due to the overlap of growth conditions for the two materials. Even if pure CNT can be grown on the template, the relatively inefficient π–π stacking between CNTs may also lead to structural collapse during the template-removal process, placing a great barrier to acquiring integral monoliths and ordered pore structures. Once these problems are overcome, such pure CNT monoliths with controlled macro- and mesopores may find great potential for a wide range of applications in catalysis, adsorption, and energy storage and conversion.

3.1.4. CNT-based Composite Monoliths

The deliberate introduction of a second component can not only strengthen the performance compared to the original 3D CNT monoliths, but may also impart some novel properties.

There is so far no report of the preparation of CNT-based composite monoliths using just the CVD process. Generally, CNT-based composite monoliths can be prepared by two methods, i.e., post-treatment of CVD-grown CNT aerogels, or a wet chemistry approach. For the first method, isotropic CNT sponges are prepared by the CVD technique as described above (see Section 3.1.2), followed by the introduction of other components to tailor them for specific applications.[70–72] For example, Chen and co-workers[71] reported a MWCNT/V_2O_5 core/shell sponge by coating pristine MWCNT sponges with a thin and uniform V_2O_5 layer via atomic layer deposition (ALD). In another work,[72] CdS nanoparticles (NPs) were anchored on a CNT sponge by dipping pristine sponges in an as-prepared CdS NP solution. The second method, i.e., the wet chemistry approach, will be introduced in the next section.

3.2. CNT-based Monoliths Derived from CNT-based Suspensions

Besides the CVD technique, CNT-based monoliths can also be derived from CNT-based suspensions (either "macrodispersions" of CNT bundles or "nanodispersions" of individual CNTs) by two steps: a sol–gel transition (or directly freezing) and a drying process. In the first step, CNT precursors (and other guest molecules) are dispersed into a solvent with/without the help of surfactants. Corresponding dispersion methods and evaluation standards have been well studied.[73–78] It should be noted that dispersion quality may have a great effect on the following gelation process and final performance of products, and this aspect has not received enough attention. After concentration or reaction, the CNT-based suspension converts to a wet gel. Conventional vacuum drying methods always produce highly aggregated xerogels with large size shrinkage, which is attributed to the dramatic surface tension change around the gel network induced by solvent evaporation.[24] To maintain the integrality of the 3D framework, either supercritical-drying or freeze-drying techniques are used to circumambulate the liquid–gas phase line of the solvent, thus producing structure-maintained aerogels (**Figure 5**).[79] Although the two drying methods usually show similar SSAs when an appropriate drying medium is used, supercritical drying always endows aerogels with higher mechanical strength. It should be noted that graphene aerogels can be prepared in a similar way,[29,58,59] hence many methods used for graphene aerogels could benefit the studies of CNT aerogels. For carbon aerogel preparation,[28,80] polymer aerogels (e.g., phenol-formaldehyde resin aerogel) are always fabricated first by chemical polymerization of multifunctional organic species followed by special drying. Then they are converted to 3D porous carbon networks by pyrolysis at high temperature, where polymers decompose to carbon particles.

Compared with the high-temperature CVD process, the wet chemistry method allows much milder synthetic conditions, which are convenient for control and scalability. More importantly, due to the decoupling of the CNT synthesis and gel assembly process, the CNT precursors and other ingredients can be well controlled or selected, thus providing large flexibility to design a wide range of materials tailoring multiple and desirable functions. However, the universal issues for wet chemistry lie in the low quality and much shorter lengths of the CNTs, which inevitably results in aerogels with limited electrical and mechanical properties.

The sol–gel step is the key procedure for preparing final products in most cases. Many sol–gel transition methods initially designed for the preparation of CNT-based wet gels can be directly applied for aerogel preparation if the second step (i.e., drying step) is added. Therefore, the sol–gel mechanism and the main approaches for preparing CNT-based wet gels are introduced in the first section below. Different types of CNT-based aerogels and some novel preparation methods are subsequently discussed.

3.2.1. CNT-based Wet Gels

Wet gels are a free-standing porous 3D solid network swollen by liquid solvent. Regarding the type of solvent, it

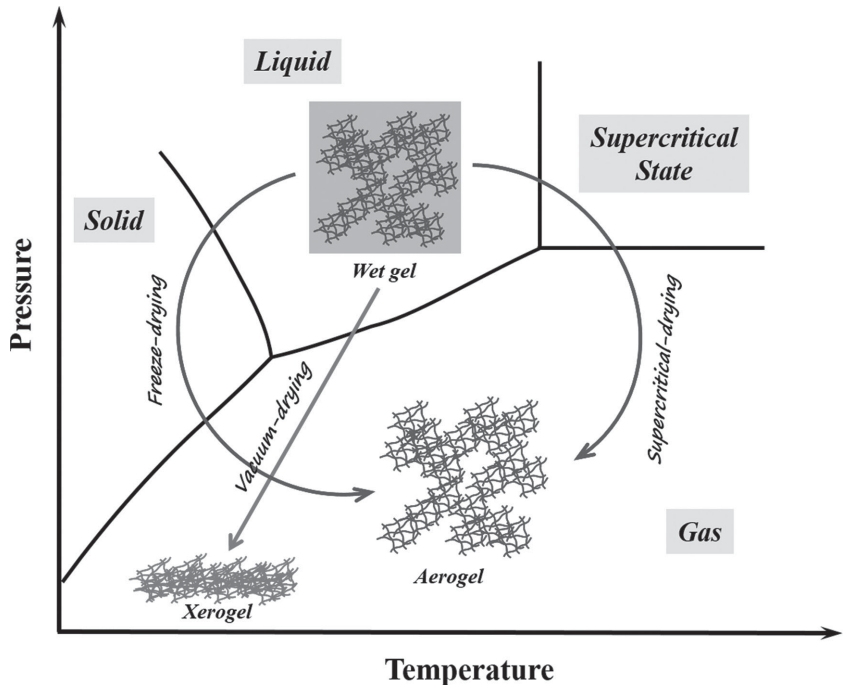

Figure 5. The phase transition from the wet gel to the dry gel. Both freeze-drying and supercritical-drying can be used to acquire an aerogel with a maintained porous 3D structure. In contrast, traditional vacuum-drying produces xerogels with large shrinkage and much lower porosity (less than 90 vol%). Reproduced with permission.[79] Copyright 2014, Wiley-VCH.

can be classified as a hydrogel (water) or organogel (organic solvent). CNT-based wet gels are prepared by crosslinking CNTs (and other polymers) in precursor solutions to form 3D networks, via either covalent or non-covalent interactions. The key points to acquire CNT-based wet gels are the achievement of a good dispersion of CNTs, the reasonable design of crosslinking forces, and the smart introduction of other functional components. The main gelation methods are depicted in **Figure 6**, where CNTs can either serve as continuous networks, partial networks, or guest components.

CNTs as Continuous Networks: Pristine or modified CNTs themselves can form 3D continuous networks with or without the assistance of dispersants. For pristine CNTs, surfactants are always employed to disperse them in water at a high concentration, thus forming a gel due to van der Waals interactions. Hough and co-workers prepared the first pristine SWCNT hydrogel using sodium dodecylbenzene sulfonate (SDBS) as a surfactant (**Figure 7**a), where the mixture exhibited gel-like behavior at 0.26 vol%, confirmed by rheology measurements.[81,82] The most exciting thing is that the surfactant could be completely removed without destroying the hydrogel,[53,83] which means that pure SWCNT gels could be obtained. Tan and co-workers reported the preparation of highly elastic SWCNT-based hydrogels using sodium deoxycholate (NaDC) at very high CNT concentrations (about 1–3 wt%).[84] As shown in Figure 7b, it seemed that the hydrogel possessed a double network, i.e., a NaDC network and a NaDC-dispersed SWCNT network, which was quite different from the previous case. As well as being dispersed with surfactants, CNTs can also form gels in organic solvents with the assistance of hydroxylamine hydrochloric acid salt via noncovalent interactions (Figure 7f).[85]

It was reported that oxidized CNTs (ox-CNTs) also exhibited gelation behavior above a critical concentration (Figure 7c), presumably due to hydrogen bonding or the topological entanglement of the rod-shaped CNTs. Ox-MWCNTs (prepared by oxidation with a mixture of concentrated nitric and sulphuric acids in a ratio of 1:3) showed a much higher gelation threshold (≈5 vol%, 8.25 wt%) than that of ox-SWCNTs (≈0.3 wt%, prepared by a

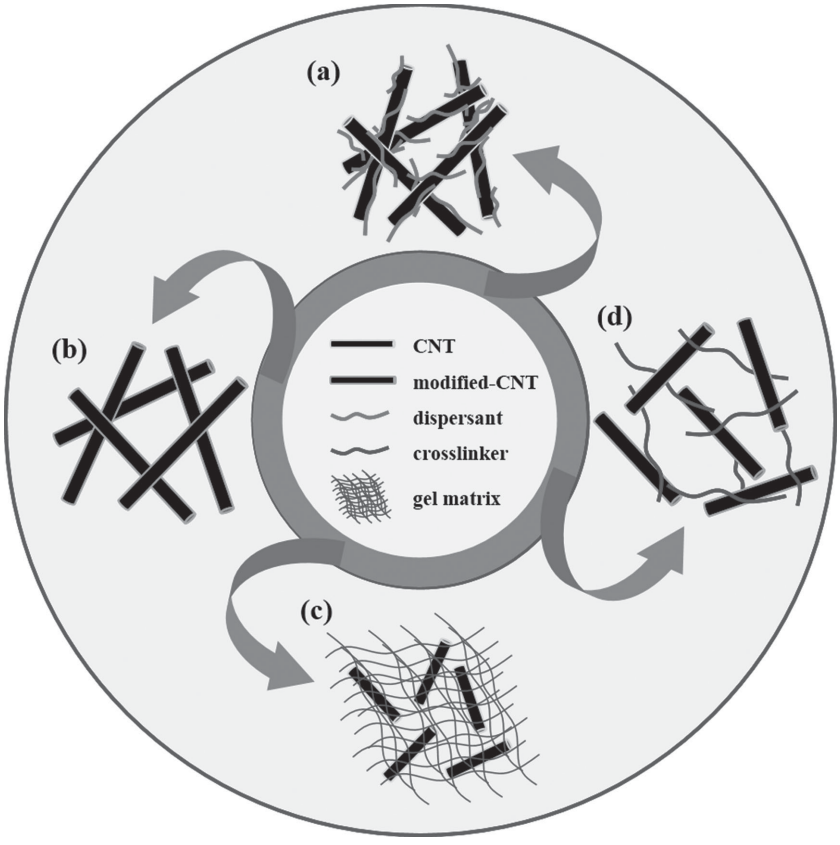

Figure 6. The schematic demonstration of general methods for preparing CNT wet gels. Formation of gels by a) suspending high-concentration pristine CNTs in solvent with a dispersant, b) dispersing high-concentration surface-modified CNTs in solvent, c) inserting CNTs into an as-prepared gel matrix, and d) crosslinking CNTs and other molecules.

modified Hummer's method).[86,87] This might be attributed to the increased crosslink points between CNTs due to the much larger SSA of SWCNTs. Even ox-SWCNT hydrogels (0.65 wt%) still showed a little viscous flow upon horizontally placing, indicating weak inter-tube interactions. In contrast, graphene hydrogels can be easily prepared from graphene oxide by hydrothermal reactions or chemical reduction.[88,89]

Super acids, such as chlorosulphonic acid, are the only true thermodynamic solvents for the dissolution of CNTs.[40,41] SWCNTs can spontaneously dissolve in chlorosulphonic acid at weight concentrations of up to 0.5 wt% by the protonation of CNTs without destroying their structures.[40] Hence it may be very promising for preparing high-quality pure CNT gels. So far, no report has centered on this method, which might be due to difficulty in handling the acid.

Combined CNTs and Other Components as Continuous Networks: In most cases, it is difficult for CNTs alone to form gels because of weak crosslinking forces (inter-tube π–π

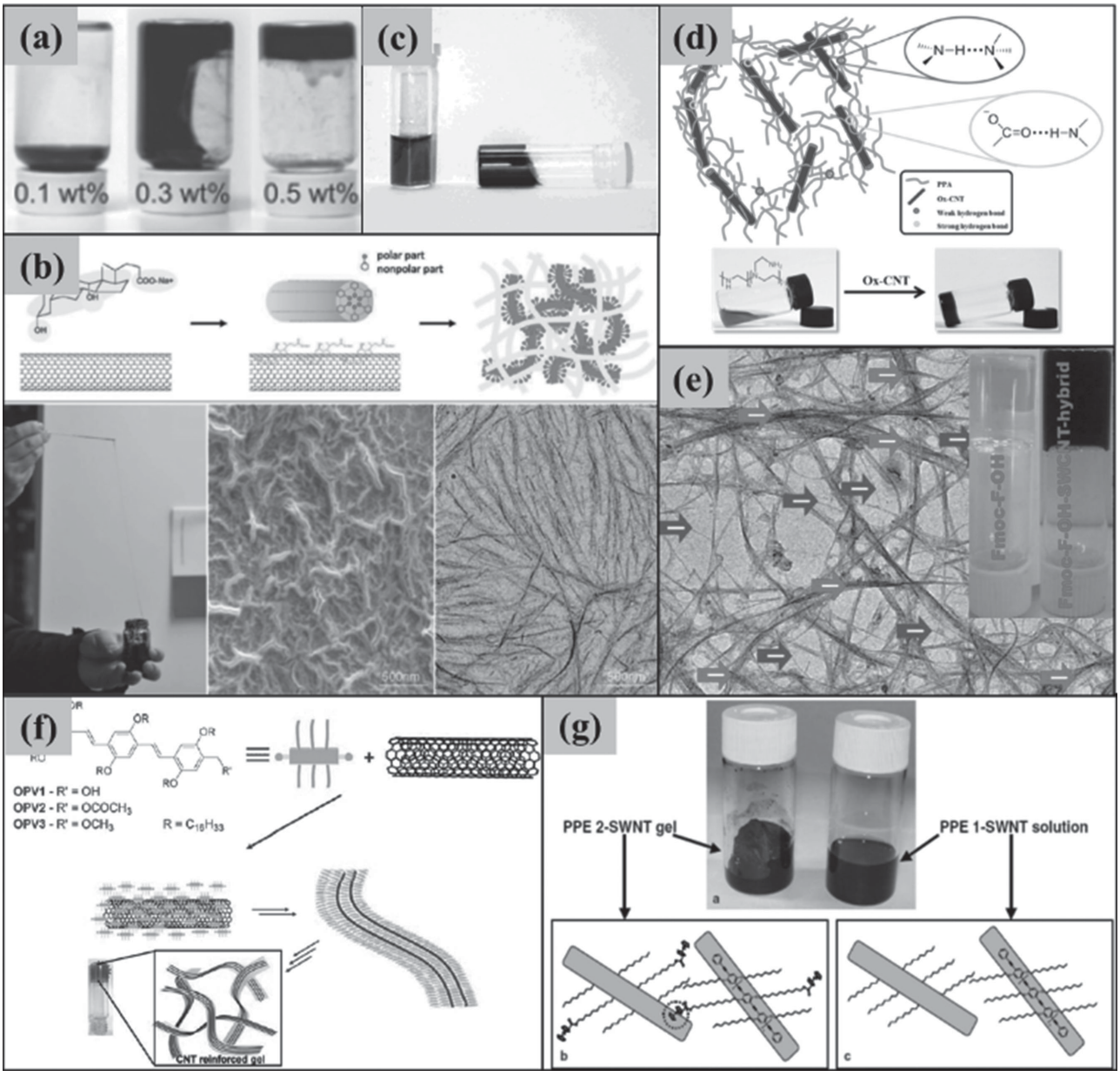

Figure 7. The demonstration of various gelation methods for preparing CNT wet gels. a,b) CNT hydrogels prepared by dispersing high-concentration pristine CNTs in water with the assistance of surfactants (SDBS and NaDC, respectively). Figure a) was reproduced with permission.[81] Copyright 2006, American Chemical Society. Figure b) was reproduced with permission.[84] Copyright 2011, Wiley-VCH. c) CNT hydrogels obtained by the condensation of oxidized SWCNT in aqueous solution at a high concentration. Reproduced with permission.[87] Copyright 2003, American Chemical Society. d) ox-MWCNT/polyethylene polyamine composite hydrogel formed by hierarchical hydrogen bonds. Reproduced with permission.[93] Copyright 2014, Wiley-VCH. e) CNT-imbedded Fmoc-protected amino acid (Fmoc-Phe-OH) hydrogel. Reproduced with permission.[105] Copyright 2012, Royal Society of Chemistry. f) Schematic representation of oligo(p-phenylene vinylene)–CNT organogel. Reproduced with permission.[96] Copyright 2008, Wiley-VCH. g) SWCNT gel obtained by crosslinking SWCNTs with ferrocene-grafted poly(p-phenyleneethynylene). Reproduced with permission.[98] Copyright 2006, Elsevier Publishing Group.

stacking) and thus a high gelation threshold. Therefore, it is natural to consider the introduction of extra components (gelation promoters) to enhance the crosslinking force. In this case, CNTs always construct 3D networks in conjunction with guest molecules. Reasonable introduction of gelation promoters can not only facilitate the gelation process, but also reduce CNT consumption (reducing the cost) and impart new functions to the hydrogels.

For example, a tertiary hydrogel was prepared by simply mixing SWCNTs, graphene oxide (GO), and poly(3,4-ethylene-dioxythiophene):poly(styrenesulfonate) (PEDOT:PSS).[90] In this system, nonfunctionalized SWCNTs were well dispersed by GO. The gelation driven force is the π–π interactions and hydrogen bonds between three components. A special case was the formation of CNT gels in an ionic liquid, where the physical crosslinking of CNT bundles could be triggered by local molecular ordering of ionic liquids.[91,92]

Sometimes, CNTs are modified to serve as crosslinkers (or gelators). Previously, we have demonstrated a multifunctional ox-MWCNT/polyethylene polyamine (PPA) composite hydrogel directed by a novel concept: hierarchical hydrogen bonding.[93] In this case, the surface of the MWCNTs was covalently modified with oxygen-containing groups by H_2SO_4/HNO_3 oxidation. By altering the proportion of ox-MWCNTs and PPA, the overall crosslinking force provided by weak hydrogen bonds (N–H···N) between PPA molecules, and strong hydrogen bonds (–COO^-···HN) between ox-MWCNTs and PPA molecules, could be continuously tuned, thus tailoring desired and multiple functions. Bayazit and co-workers[94] reported that pyridine-functionalized SWCNTs can serve as gelators to gel poly(acrylic acid) (PAA), where the gel was formed from hydrogen bonding between pyridine and carboxylic acid groups. Another interesting work was presented by Cheng and co-workers, where SWCNTs wrapped with special DNA (leaving the sticky domains pointing out) were synthesized as gelators to interact with linear unit DNA (duplex DNA with two sticky domains) for constructing a 3D network.[95] In this case, reversible gelation behavior could be realized by altering the pH. When the pH was lower than 6.3, two sticky domains could form an intermolecular i-motif structure via the formation of C···CH^+ base pairs, thus affording gelation, and vice versa. Some CNT-based gelators used in organic solvents have also been developed (Figure 7g).[96–98]

CNTs as Guest Components: In another type of gel, CNTs are used as guest components to enhance the properties (e.g., mechanical strength, electrical conductivity) of the original gel matrix. In this case, CNTs often have little effect on gel formation.[99–105] For example, with the assistance of Pluronic copolymer, SWCNTs were dispersed and incorporated in the supramolecular hydrogel matrix constructed by Pluronic copolymer and α-cyclodextrin (α-CD).[100] It was also shown that NaDC-dispersed SWCNTs could be inserted into the poly(*N*-isopropylacrylamide) (pNIPAM) hydrogel matrix, greatly accelerating the thermal response process.[104]

3.2.2. Pure CNT Aerogels

Preparation of pure CNT aerogels is of great importance to fully realize their exceptional performance (without the introduction of inert components) and to study the intrinsic properties of CNTs. Most of the wet gels mentioned above can be directly converted to the corresponding aerogels by a special drying process such as freeze-drying and supercritical drying. However, pure CNTs wet gels are very difficult to prepare. Hence, the fabrication of the corresponding pure CNT aerogels remains a big challenge.

One method to get pure CNT wet gels is to disperse pristine CNTs with surfactants and then wash them off, which was described in previous section (SDBS-dispersed CNT hydrogels). Based on this method, Bryning and co-workers reported the first few-walled CNT (FWCNT) aerogel supercritical drying of SDBS-dispersed CNT hydrogels (**Figure 8**a,b).[53] Thanks to the less destructive dispersing conditions (without the oxidation of CNTs), the resultant low-density (10–30 mg mL^{-1}) aerogels showed a high conductivity (up to 1 S cm^{-1}). However, unlike CVD-grown CNT sponges, the as-prepared CNT aerogels were fragile because of reduced covalent bonding (chemical bonds in an individual CNT) and increased physical interactions (inter-tube van der Waals interactions and π–π stacking), resulting from the short length of the individual CNTs. By replacing FWCNTs with SWCNTs, the surface area of the aerogel reached 1291 $m^2\ g^{-1}$, approaching the theoretical limit (1315 $m^2\ g^{-1}$) of SWCNTs.[106] This result strongly suggests the potential of using the aerogel form to fully exert the remarkable properties of CNTs.

Jung and co-workers developed another intriguing and general approach for gelling surfactant-suspended SWCNT dispersions (Figure 8c).[107] The diluted SDBS-suspended SWCNT dispersion was concentrated in a controlled way by evaporation under mild conditions (313 K). Finally, gelation occurred with increased van der Waals interactions between contacting SWCNTs at the transition region between semi-dilute and isotropic concentration regimes. The corresponding aerogels obtained by supercritical drying showed a very low density (2.7 mg cm^{-3}), a high surface area (1011 $m^2\ g^{-1}$), and good electrical conductivity (0.91 S cm^{-1}). The most exciting point is that this method allows a low initial CNT concentration (less than 0.1 wt%), greatly reducing the difficulties in suspension preparation, and may thus largely maintain the remarkable properties of CNTs. Additionally, it is also a very general method for preparing aerogels with other 1D and 2D nanostructured building blocks (e.g., Ag nanowires, MoS_2 nanosheets).

3.2.3. CNT-based Composite Aerogels

To facilitate the gelation process and impart additional properties to the materials, CNTs are always mixed with other components to produce wet gels and corresponding aerogels. Unlike solely inter-tube physical interactions for pure CNT aerogels, many types of covalent and noncovalent crosslinking forces are involved in CNT-based composite aerogels. Therefore, rich alternative interactions can be used to efficiently manipulate the gelation behavior, introducing diverse structures and functions in resultant materials. In this section, different types of CNT-based composite aerogels with CNTs, nonCNT components, and both of these as continuous networks are introduced in turn.

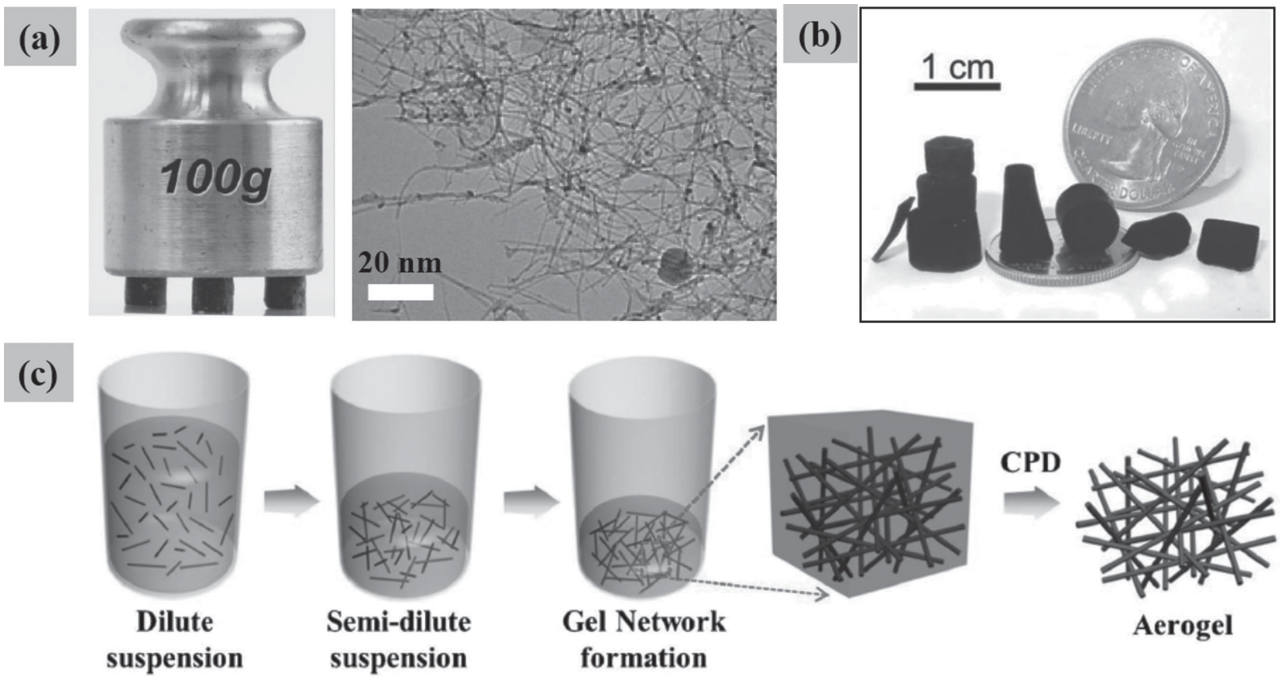

Figure 8. Pure CNT aerogels derived from wet chemistry methods. a,b) CNT aerogels obtained from supercritical drying of CNT hydrogels produced from SDBS-suspended CNTs in aqueous solution. Figure a) was reproduced with permission.[53] Copyright 2007, Wiley-VCH, Figure b) was reproduced with permission.[106] Copyright 2013, Wiley-VCH. c) Schematic representation of CNT aerogels produced from their colloidal suspensions by gradual evaporation of the solvent. Reproduced with permission.[107] Copyright 2012, Nature Publishing Group.

CNTs as Continuous Networks: Composite aerogels with CNTs as continuous networks can not only utilize the well-defined conductive paths and large specific surface areas provided by inter-connected CNTs, but can also trigger new properties by the introduction of guest components. For example, Worsley and co-workers showed that many metal oxides, such as SiO_2, SnO_2, and TiO_2, can be uniformly coated onto SWCNT-based carbon aerogel (SWCNT-CA) scaffolds by a facile sol–gel deposition process (**Figure 9**a).[108]

CNTs and Other Components Combined as Continuous Networks: When gel networks are constructed by the combination of CNTs and other components, the crosslinking forces can be tailored for specific applications.[109–112] For example, Zhang and co-workers[112] demonstrated a dendrimer-linked CNT aerogel via hydrogen bonding between carboxylic acid groups on ox-CNTs and amino groups on amino-terminated generation 5-poly-(amido amine) (PAMAM). Thanks to the pH-sensitivity of hydrogen bonds, the aerogel showed a reversible sol–gel transition behavior, enabling its use as a recyclable adsorbent for dye stuffs. In another work,[109] CNTs were dispersed in chloroform with the assistance of ferrocene-grafted polymers, then the polymer-wrapped CNTs served as gelators to form wet gels via the π–π interactions between ferrocenyl groups and neighboring CNT surfaces (Figure 7g). Wet gels were further converted to aerogels after supercritical drying (Figure 9c,d). It is worthy to note that the electrical conductivity and surface area of as-prepared composite aerogels can be remarkably enhanced by a post-synthetic thermal annealing process in air, which allowed their use for energy-related applications.

To strengthen the crosslinking forces (by acquiring more efficient π–π stacking) and application performance, graphene is introduced.[113–115] Based on the good dispersing ability of graphene oxide (GO) for CNTs, either pristine CNTs or functionalized CNTs can form uniform suspensions with the assistance of GO. The wet gel can be consequently obtained via chemical reduction or hydrothermal reduction,[114,115] then turned into an aerogel after special drying. In this system, graphene and CNTs jointly construct 3D networks, always with graphene providing a large SSA and CNTs providing the conductive pathway. Additionally, it was believed that CNTs could serve as spacers to suppress the stacking of graphene flakes and thus promoting the overall surface area.

Interestingly, the formation of wet gels is not a prerequisite for obtaining aerogels. Sometimes, freeze drying frozen solutions can directly give rise to free-standing aerogels. It was reported that polyvinylalcohol (PVA)-dispersed CNT suspensions can be directly converted into aerogels via flash-freezing followed by lyophilization.[116] In this system, PVA serves as both a dispersant for CNTs and a structure holder for the aerogel. Another amazing composite aerogel was reported by Sun and co-workers in 2013,[117] where graphene/CNT aerogels were acquired by simply freeze drying mixed giant graphene oxide (GGO) and acid-treated MWCNTs in water followed by hydrazine vapor reduction. Due to the synergistic effect between elastic CNT ribs and giant graphene cell walls, the aerogels showed ultralow apparent densities (≈0.16 mg cm^{-3}) and extraordinary reversible compressibility.

CNTs as Guest Components: Inserting CNTs into preformed monolithic 3D networks (e.g. silicon aerogels,

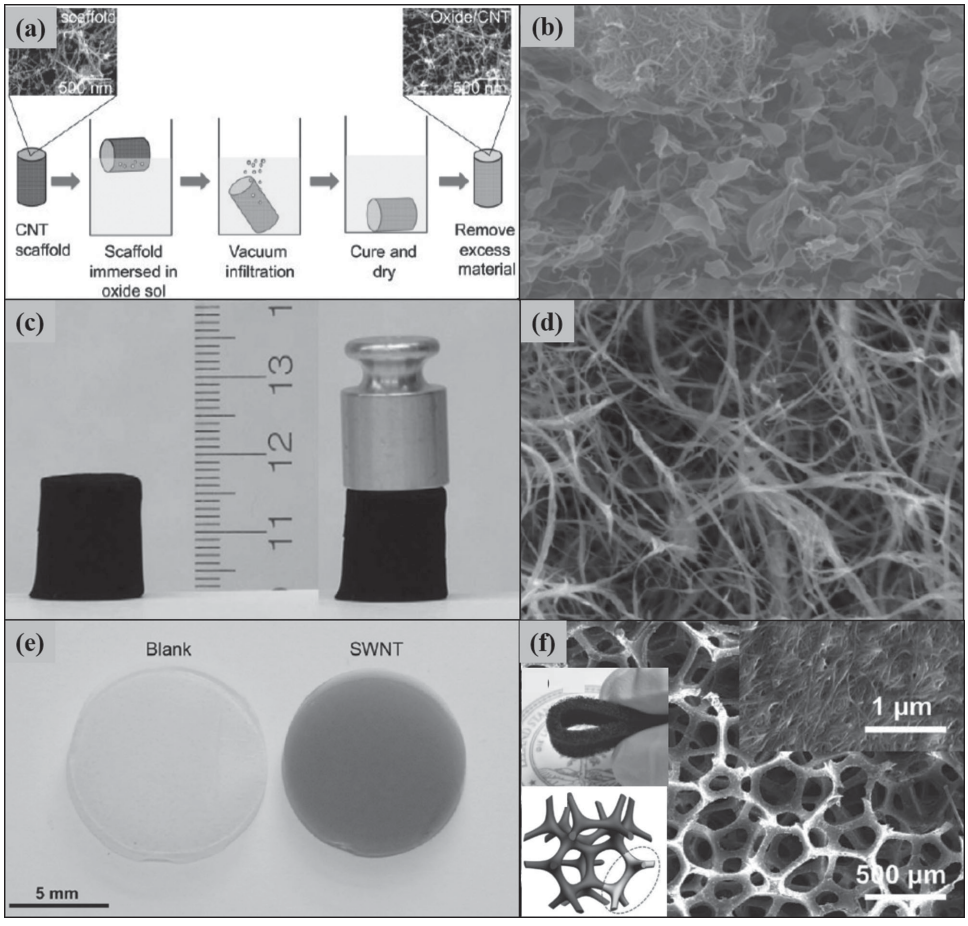

Figure 9. Some examples of composite CNT-based aerogels. a) CNT/oxide composite aerogels with CNTs as scaffolds. Reproduced with permission.[108] Copyright 2011, American Chemical Society. b) A scanning electron microscope (SEM) image of a PVA/MWCNT aerogel containing 50 wt% MWCNTs. Reproduced with permission.[116] Copyright 2011, Elsevier Publishing Group. c,d) A digital photo and SEM image of ferrocene-grafted poly(p-phenyleneethynylene)-crosslinked CNT aerogels. Reproduced with permission.[109] Copyright 2011, Elsevier Publishing Group. e) Silica aerogels without and with SWCNTs. Reproduced with permission.[121] Copyright 2011, American Chemical Society. f) CNT-coated macroporous sponges. Reproduced with permission.[125] Copyright 2012, Royal Society of Chemistry.

phenol-formaldehyde resins, polymers) can enhance the performance or impart additional functionality to the original materials.[118–121] As additives, the proportion of CNTs is always much smaller than that of the gel matrix. For example, incorporating functionalized FWCNTs into a nanofibrillated cellulose (NFC) gel matrix can dramatically enhance the electrical conductivity of the aerogel by several orders of magnitude.[120] CNT-containing carbon aerogels have also been reported,[118,119] where suspended CNTs were involved in the matrix of phenol-formaldehyde resin by in-situ polymerization and post-carbonization processes at high temperature. After thermal treatment, CNTs were connected by the carbon particles from decomposed polymers, thus achieving exceptional electrical conductivity (>10 S cm^{-1}) and Young's moduli (>10 MPa) at a high aerogel density (e.g., >300 mg cm^{-3}).[119]

In the above examples, the CNTs were randomly distributed in the 3D networks. Due to their relatively low fraction, CNTs may not be able to form continuous works and thus the enhancement efficiency is affected. Regarding this, a great idea came: surface-coating the continuous 3D matrix with CNTs.[122–125] For instance, Petrov and co-workers[123] coated the as-prepared macroporous poly(*N*-isopropylacrylamide) (PNIPAAm) cryogel with a thin layer of CNTs by an ice-mediated process. During this process, the chemical-crosslinked macroporous PNIPAAm cryogel was immersed in a CNT suspension, then CNTs were forced to deposit on the pore walls of the cryogel during lyophilization. Thanks to the interconnected CNTs on the gel surface, the nanocomposite exhibited a high conductivity ≈10^{-2} S m^{-1} with only 0.12–0.15 wt% CNTs. In a more recent work, Xie and co-workers[125] presented a CNT-surface-modified polyurethane sponge obtained by an extremely simple approach, i.e., dipping the sponge in a CNT ink and drying at ambient pressure (Figure 9f). Thanks to the macroporous structure and excellent mechanical properties of the polyurethane sponge, the modified sponge showed both superior conductivity (≈1 S cm^{-1} with a CNT coating of ≈200 nm thick) and mechanical properties (e.g., stretchability and compressibility).

3.2.4. CNT-based Aerogels Derived from Other Approaches

Apart from the methods described above, some recently developed strategies, not limited to this field, may provide new ideas for designing CNT-based aerogels.

The mechanical properties of aerogels can be dramatically enhanced by the combination of dry and wet chemistry methods. Kim and co-workers[113] obtained graphene-coated CNT aerogels by preparing the CNT hydrogels via wet chemistry and further coating graphene on it via dry chemistry methods (**Figure 10**a). In brief, they dipped the pre-formed CNT hydrogels into a polyacrylonitrile solution, followed by a two-step pyrolysis to convert the polymers into graphene flakes. In this way, the graphene coating significantly strengthened the CNT struts and crosslinking nodes. Therefore, the composite aerogel not only had a six-fold improvement of the Young's modulus compared to the original CNT aerogel, but also exhibited superior elasticity (with nearly no mechanical deterioration after 2000 cycles at 60% strain), which originated from the enhanced recovery force. The amazing mechanical properties of this graphene-coated CNT aerogel may also benefit from the less destructive method of hydrogel preparation and the formation of carbon-based linkers (either graphene flakes or carbon nanoparticles) between CNTs during post-synthetic pyrolysis.

To create nitrogen-doped and highly conductive CNT aerogels, we have developed a general method based on an "erasable" promoter-assisted hydrothermal reaction coupled with pyrolysis (Figure 10b).[126] In this manner, the small-sized pyrrole bearing two functional groups (an aromatic ring and a hydrogen donor) was used to strengthen the crosslinking force between oxidized MWCNTs (ox-MWCNTs). With the pyrrole as a built-in nitrogen source, the composite hydrogel was converted into a nitrogen-doped CNT aerogel through subsequent supercritical drying and pyrolysis steps. In the pyrolysis step, besides nitrogen doping, extra pyrrole molecules were removed by either evaporation or decomposition due to their small size. The electrical conductivity of the aerogels could also be remarkably restored (10.9 S m^{-1}) due to the thermal reduction of ox-MWCNTs. Therefore, the resultant clean and highly conductive N-CNT aerogels exhibited exceptional oxygen reduction reaction (ORR) catalytical performance in alkaline media, with a positive onset potential of -0.055 V (versus AgCl/Ag) and a dominant four-electron pathway. Most importantly, due to the decoupling of CNT synthesis and gel preparation, and the smart use of bifunctional small molecules, this method provided great flexibility to create a variety of heteroatom-doped CNT aerogels with different types of CNTs (i.e., number of walls, chiralities) and different doping elements.

Elaborate design of the drying process can significantly modulate the morphology and corresponding properties of CNT aerogels. It was found that rapid cooling (by liquid propane) of nanofibrillated cellulose/FWCNT hydrogels produced a fibrous aerogel skeleton, while slow cooling by liquid nitrogen resulted in an interconnected sheet morphology.[120] Alignment structures with tailored macropore sizes can also be achieved by special design of the drying process.[127–130] For example, Zou and co-workers[130] acquired poly(3-hexylthiophene)-*b*-poly(3-(trimethoxysilyl) propyl methacrylate (P3HT-*b*-PTMSPMA) crosslinked MWCNT aerogels with honeycomb-like macropores by unidirectionally freezing corresponding wet gels followed by lyophilization. The unique aligned pore structures endowed aerogels with anisotropic mechanical properties and high compressibility.

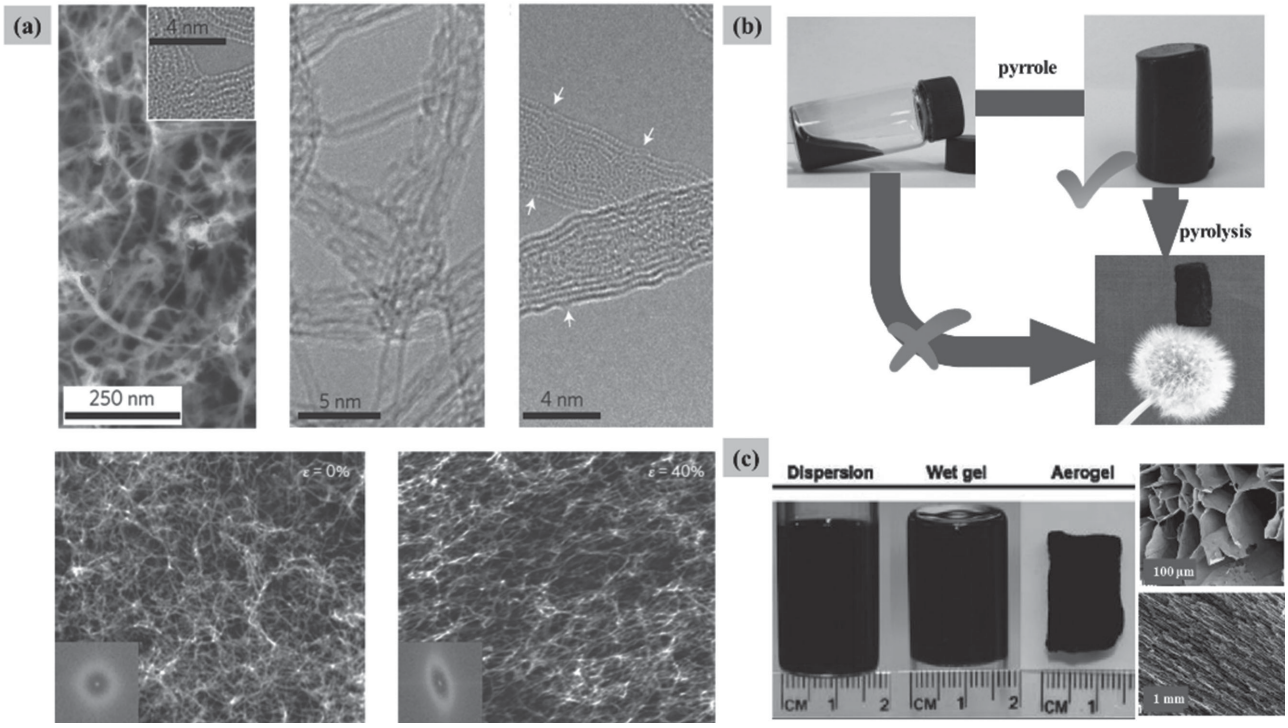

Figure 10. Examples of CNT-based aerogels produced by novel methods. a) TEM and SEM images of graphene-coated CNT aerogels. Reproduced with permission.[113] Copyright 2012, Nature Publishing Group. b) Schematic demonstration of N-doped CNT aerogels created by an "erasable" promoter-assisted hydrothermal reaction coupled with pyrolysis. Reproduced with permission.[126] c) Chemical crosslinked MWCNT aerogels prepared by ice segregation-induced self-assembly (ISISA). Reproduced with permission.[130] Copyright 2010, American Chemical Society.

There are some other interesting novel strategies in other fields which may benefit the preparation of CNT aerogels. From the point of view of wet gel preparation, electrophoretic adhesion of oppositely charged components,[131] and dynamic chemical bonds (e.g., Schiff base linkages[132] may provide some hints to creating functional CNT-based hydrogels (e.g., hydrogels with a self-healing behavior). From the standpoint of structural control, the method of oil-droplet templating used in graphene aerogel preparation may give us some inspiration.[133,134] In this case, elaborate control of the soft template can create desired macropores, and thus confer an extremely low density (≥1 mg cm^{-3}) and high compressibility on the resultant aerogels. As another example, high-cost special drying methods (e.g., freeze drying and supercritical drying) were avoided in aerogel preparation. For graphene-based aerogels, at least two recent works claimed that drying under ambient conditions might be a better choice for special applications of aerogels, such as supercapacitors with high volumetric capacitance.[135,136] Surprisingly, one work showed that the specific surface area of the resultant material from ambient-condition drying was even comparable to that of freeze-dried samples.[135]

To date, the uniqueness of CNTs has far from been exploited. For instance, CNT aerogels constructed by exclusively metallic SWCNTs should enjoy remarkable performance in catalysis and supercapacitors because of their much-enhanced conductivity. Manipulation of CNT chiralities, lengths, and diameters in aerogels may also lead to some interesting or high-performance materials for the fields of separation, electronics, and structural materials. There is a huge amount of things which remain to be explored for CNT-based aerogels, and numerous opportunities are waiting for scientists in broad communities.

4. Characterization and Application of CNT-based 3D Monoliths

After aquiring CNT-based 3D monoliths, it is essential to select approprite characterization methods to determine their structures, physicochemical properites, and application potentials. Based on this information, one can revisit the original design and devise superior aerogels relevent to specific applications. The physical properties of some typical CNT-based aerogels are listed in **Table 1**. In this section, we will first give a brief introduction of frequently used characterization methods for evaluating CNT-based aerogels, then some main applications, such as

Table 1. Physical properties of some typical CNT-based aerogels.

Material	Fabrication Method	Density [mg cm^{-3}]	Specific Surface Area [m^2 g^{-1}]	Electrical Conductivity [S cm^{-1}]	Ref.
CNT aerogel muscles	drawn from MWCNT arrays	1.5	/	/	[170]
CNT sponge	CVD	≈5–10	62.8	≈1.7 (two-probe)	[55]
CNT sponge	CVD	≈5–25	/	≈0.83 (two-probe)	[70]
Ultralong VA-CNT array	CVD	/	/	/	[57]
B-doped CNT sponge	CVD	≈10–29	360.4	/	[65]
N-doped CNT sponge	CVD	≈30–55	/	≈0.15–0.21 (four-probe)	[66]
Graphene-coated CNT aerogel	sol–gel and pyrolysis	14	/	≈0.3 (two-probe)	[113]
CNT/G foam	CVD	6.9	/	/	[67]
CNT/G foam	CVD	/	497	/	[69]
SWCNT aerogel	sol–gel	≈7.3–13.1	up to 1291	≈0.23–0.71 (two probe)	[106]
SWCNT aerogel	sol–gel	2.7	1011	0.91 (four probe)	[107]
SWCNT/DWCNT aerogel	sol–gel and pyrolysis	≈7–16	590–680	≈1–2 (four probe)	[109]
SWCNT/carbon aerogel	sol–gel and pyrolysis	30	162	1.1 (four-probe)	[108]
SiO_2/SWCNT/carbon aerogel	sol–gel, pyrolysis and infiltration	80	742	1	[108]
Graphene–MWCNT hybrid aerogel	sol–gel	42	435	0.075 (four-probe)	[114]
Dendrimer-linked MWCNT aerogels	sol–gel	≈12–14	≈182–196	/	[112]
PTMSPMA-crosslinked MWCNT aerogel	sol–gel	4	580	up to 0.26 (four-probe)	[130]
Streptavidin–biotinylated/SWCNT aerogel	sol–gel	0.4	/	/	[111]
MWCNT/chitosan/Pt NPs	ISISA	/	/	Up to 2.5	[127]
MWCNT/graphene composite aerogels	freeze-drying	≥0.16	≈272	≈0.6	[117]
N-doped CNT aerogel	sol–gel and pyrolysis	≈13.4–92.5	≈356–867	up to 0.11 (two-probe)	[126]
FWCNT-modified native nanocellulose aerogels	sol–gel	≈10–54	/	up to 1.8 (four-probe)	[120]
DWCNT-contianing carbon aerogels	sol–gel	≈139–231	≈550–590	≈5.0–8.1 (four-probe)	[118]
CNT-coated macroporous sponge	infiltration	/	≈104 m^2 m^{-3}	≈1 (not mention)	[125]
MnO_2–CNT—sponge	infiltration and electrochemical deposition	/	174	/	[122]
PNIPAAm-cryogel/SWCNT	ice-mediated deposition	21	/	2.8×10^{-4} (four-probe)	[128]

catalysis, energy storage, adsorbents, and sensors, will be introduced.

4.1. Characterization

The characterization methods for CNT aerogels can be roughly divided into four classes, based on what is being characterized: individual CNT quality, chemical composition, pore structure, or application properties. The details of the characterization of CNTs have also been reviewed elsewhere,[3,32,137,138] hence herein we just give a relatively brief introduction of characterization methods that are useful for CNT-based 3D monoliths.

4.1.1. CNT Quality Characterization

The quality of individual CNTs can greatly affect the macroscopic properties (e.g., mechanical, electrical) and application performances of CNT-based aerogels. Typically, the CVD method creates CNT aerogels with high-quality CNTs (long length and few defects), while wet chemistry methods always produce short CNTs (less than 1 μm) with many defects (e.g., oxygen-containing groups, holes).

The length of CNTs can be facilely determined by SEM, although the entanglement of CNTs may make it difficult to get accurate results. Defects on CNT surfaces can be directly imaged by high-resolution transmission electron microscope (TEM). Raman spectra, electron energy loss spectroscopy (EELS), and X-ray photoelectron spectroscopic (XPS) are also capable of determining the quality of CNTs. The G-band-to-D-band ratio in Raman spectra reflects the disorder in the carbon lattice (smaller G/D ratios represent larger disorder degrees), while EELS and XPS can evaluate the bonding state and the proportion of carbon element. The solid-state nuclear magnetic resonance and UV–vis spectra used for the characterization of the disorder degree of GO[139] may also be applied to the quality evaluation of CNTs.

4.1.2. Chemical Composition Characterization

Chemical compositions can partially reflect the quality of CNTs (always from the carbon/oxygen ratio), identify the remaining metal impurities, and evaluate heteroatom doping in CNT aerogels.

XPS is widely used to analyze the chemical composition of CNT-based aerogels, so as to obtain information about the functional groups, heteroatom-dopant mode/content, and the metal residues. Although XPS can analyze most elements in the periodic table, it can only give surface information and may thus lead to some errors. To get the bulk chemical composition information (mainly for C, H, O, N, S, P), elemental analysis by an elemental analyzer may be a better choice. Apart from the chemical composition analysis, energy-dispersive X-ray analysis (EDX) and EELS can further give space-resolved composition information about aerogels, useful to evaluate the distribution of heteroatoms or metallic elements in the 3D network.[65] However, it should be noted that the detection sensitivity of XPS, EDX, and EELS are not capable of identifying trace amounts of metal residues in aerogels introduced by CNT growth or post treatments. In this regard, inductively coupled plasma mass spectrometry (ICP-MS) may serve as a more powerful tool to solve this problem, with its high resolution at the ppb level.[140,141]

In addition, spectral methods such as IR spectroscopy can also provide some indirect information about the chemical composition from characteristic peaks. Heteroatom doping, such as nitrogen doping of SWCNTs, can also be identified by Raman spectra, where N-doping causes a red shift of the G' band.[142] By correlating the spectral information (e.g., peak intensity, peak shift) with the chemical composition as determined directly by elemental analysis, one may get the chemical composition information from the spectra.

4.1.3. Pore Structure Characterization

The pore structure of CNT-based aerogels is critical for their application performance. The main indices for evaluating pore structure are the pore size distribution (PSD), the specific surface area (SSA), and the porosity.

According to the definition given by IUPAC,[143] typical CNT-based aerogels possess abundant macropores (diameter: >50 nm) and mesopores (diameter: ≈2–50 nm) which can be directly imaged by SEM or TEM. Nitrogen adsorption measurements are the most important method to probe both the SSA and PSD. As the mesopores are crucial for most applications of aerogels, the Brunauer–Emmett–Teller (BET) method and Barrett–Joyner–Halenda (BJH) method are frequently used to analyze SSA and PSD, respectively. For some special micropore-containing aerogels, data in the low p/p_0 region should be recorded and the nonlocalized DFT (NLDFT) method and the t-plot method may be used to give reasonable results.[79]

Porosity is another important factor for evaluating porous CNT-based aerogels. The porosity can be calculated as $\varphi = (1\text{-}\rho_{aerogel}/\rho_{CNT}) \times 100\%$, where $\rho_{aerogel}$ and ρ_{CNT} represent the apparent densities of the aerogel and of the CNTs, respectively.[120] The densities of different types of CNTs have been determined experimentally or theoretically,[144,145] hence, the porosity (typically >95%) can be easily obtained by measuring the apparent density of the aerogel.

4.1.4. Characterization of Properties for Applications

For practical applications, many physicochemical properties including thermal, mechanical, electrical, and electrochemical properties of CNT-based aerogels need to be characterized so as to find the most relevant application fields for these materials.

Based on CNT aerogels derived from SDBS-suspended aqueous CNT dispersions, Islam and co-workers applied much effort in thermal property studies both via experiments and theoretical calculations.[83,106,146] For example, they found that the junction thermal conductance in the SWCNT aerogels approaches the theoretical maximum for a van der Waals-bonded SWCNT junction.[146] Interestingly, they found

that the low-density SWCNT aerogel, which was expected to be a thermal insulator (as is the case for silica aerogels), showed a good heat transfer ability (**Figure 11**a).[106] This might be due to the ultrahigh thermal conductivity of individual SWCNTs (≥1000 W m^{-1} K^{-1}) and the well-connected 3D networks.

For mechanical properties, most work has focused on the compressible property of aerogels, carried out by a universal testing machine. From stress–strain curves, one can obtain the compressive modulus (the slope of the curve), the compressive strength (the stress when the material was broken), the energy dissipation efficiency (the area of hysteresis loops), and the compressible reversibility.[55] Some work was also conducted using dynamic measurements by dynamic thermomechanical analysis (DMA), which gives information about the elastic modulus (storage modulus E' and loss modulus E'') and the temperature-dependent mechanical properties.[65,113,117] As an example, Kim and co-workers greatly improved the mechanical properties of CNT aerogels by graphene-flake coatings, and studied the reinforcement mechanism involved.

High electrical conductivity is important for many applications including sensors, catalysis, supercapacitors, and so on. Electrical conductivity has always been calculated from I–V curves obtained by two-probe[53] or four-probe[107] methods. Due to the porous nature of aerogels, the contact region between the sample and the probe was always painted with a little conductive paint, so as to get a more effective contact with the probe. The obtained conductivity using the four-probe method was always higher than for the two-probe method, because the former can eliminate contact resistance between the probe and the sample.[147] However, due to the difference in aerogel densities, we recommend that the bulk density should be displayed when comparing the electrical conductivity of different samples.

The most effective method to evaluate the potential of CNT-based aerogels for capacitors, batteries, and electrocatalysis is the electrochemical measurement via an electrochemical work station or specific battery test system. For electrochemical energy storage and conversion devices, cyclic voltammetry (CV) and galvanostatic charge–discharge curves are currently adopted, using different scan rates or current densities so as to to probe the capacitive properties, including the mass/area-based specific capacity and rate performance (capacities versus scanning rates or current densities).[148,149] Since the energy density and power density are two main factors in energy-storage devices, sometimes Ragone plots (recorded energy density versus power density in a single device) are required to evaluate the practical application properties, where the available energy at a constant power load can be clearly demonstrated.[150] It should be noted that measurements using two-electrode or three-electrode configurations can give very different results. The former method is considered more appropriate to estimate the capacitance for practical applications. The pros and cons of the two methods have been well reviewed by Stoller and co-workers.[151]

For electrocatalysis, CV and linear sweep voltammetry (LSV) are often used to evaluate the catalytic activity. The onset potential, half-wave potential, and catalysis current densities are some critical parameters for almost all types of electrocatalysis. Some complex reactions involving multiple phases (e.g., the oxygen reduction reaction) require more complex equipment, such as a rotating disk electrode (RDE) or rotating ring–disk electrode (RRDE) to enhance the mass transfer and study the reaction mechanism.[149] For both electrochemical energy storage and catalysis, electrochemical impedance spectroscopy (EIS) and current–time (*I–t*) curves (or repeating CV curves) are often used to evaluate the electron transfer resistance and the stability of the electrode materials, respectively. Some derivative diagrams, such as Tafel plots, are also useful to get further information about the catalytic mechanism.

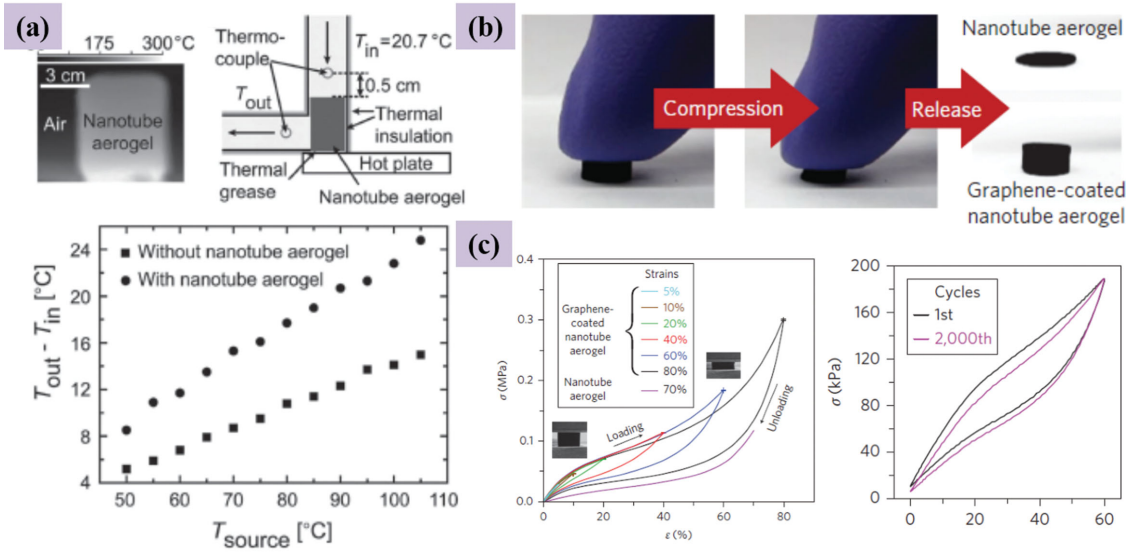

Figure 11. a) The thermal management characteristics of SWCNT aerogels. Reproduced with permission.[106] Copyright 2013, Wiley-VCH. b,c) The mechanical (superelastic and anti-fatigue) properties of graphene-coated CNT aerogels. Reproduced with permission.[113] Copyright 2012, Nature Publishing Group.

4.2. Applications

Thanks to the incredible properties inherited from the parent aerogels (hierarchical open pores, high porosity, low density, etc.) and individual CNTs (high theoretical SSA, mechanical flexibility, mechanical strength, ultrahigh conductivity, fully-conjugated structure, diverse structure-dependent properties, etc.), CNT-based aerogels exhibit promising application potential for diverse fields (**Figure 12**). Main applications of CNT-based aerogels are introduced in this section. It should be noted that until now, almost all applications of CNT aerogels overlap that of graphene aerogels. The further improvement of application performance and expansion of application territory require ingenious utilization of unique tubular geometry and structural diversities of CNTs.

4.2.1. Energy Storage

Highly efficient electrode materials for energy storage require some general principles, such as high electrical conductivity for rapid electron transfer (high power density), hierarchical open pores for fast mass transfer (high power density), a high SSA for more accessible reaction sites (high energy density), and high stability (e.g., chemical, mechanical) for a long shelf life and cycle life. Considering these factors, CNT-based aerogels seem to be a superb material in this field. However, the performance of current CNT-based aerogels cannot rival all materials, for example, graphene-based aerogels. Enormous efforts are needed to investigate the structure–performance relationship of CNTs, and to develop efficient methods for purposefully preparing CNT-based aerogels with controlled individual CNT structures, large SSAs, suitable pore size distribution, and appropriate additives.

Many efforts have been made regarding the use of CNT-based aerogels as electrode materials for supercapacitors.[69,115,122,124,152] For supercapacitors, energy density is always the limiting factor. The energy density of a packed cell can be written $E = 0.5CV^2$, where C is the total specific capacitance in the circuit and V is the cell voltage.[152] Hence, from the point of view of electrode materials, a high specific capacitance is desired. The total capacitance is made up of the electrical double-layer capacitance (EDLC) and pseudocapacitance. The energy storage mechanism for EDLC lies in the physical adsorption of opposite ions at the electrode–electrolyte interface during charging, where hierarchical pores (mesopores and macropores) and large surface areas for electrolyte ion penetration and adsorption are required. In this case, the CNT-based aerogel not only provides a large SSA for a high gravimetric energy density, but also provides interconnected conductive networks for fast electron transfer, which enables fast charging/discharging processes throughout the entire 3D network. In other words, the energy storage should be scaled up by directly increasing the thickness of the electrode material without losing power density. Some works, e.g., research into CNT/graphene aerogels, have focused on the promotion of EDLC by improving the specific surface area,[69,115] where CNTs can suppress the stacking of graphene flakes and provide extra conductive paths. In this strategy, the specific capacitance can reach ≈286 F g^{-1} at 1.78 mA cm^{-2} when using nickel foam as current collector.[69] Although a high stability, high rate performance, and moderate capacity can be achieved using pure EDLC with exclusively carbon-based materials, further improvement of the capacitance is required for obtaining a high energy density. For this purpose, pseudocapacitance, where the capacitance is provided by a reversible redox reaction during the charging/discharging process, is introduced. A common method is to make composite CNT-based aerogels by integrating conductive CNTs with other components that possess a large pseudocapacitance (e.g., metal oxides and conducting polymers). For example, Chen and co-workers[122] reported a MnO_2–CNT sponge supercapacitor (**Figure 13**a). The macropores in the sponge enable the fast transfer of electrolyte ions, CNT coatings provided chemical inertness and high conductivity for fast electron transfer, and the MnO_2 provided a large pseudocapacitance (theoretically 1370 F g^{-1}). Based on this

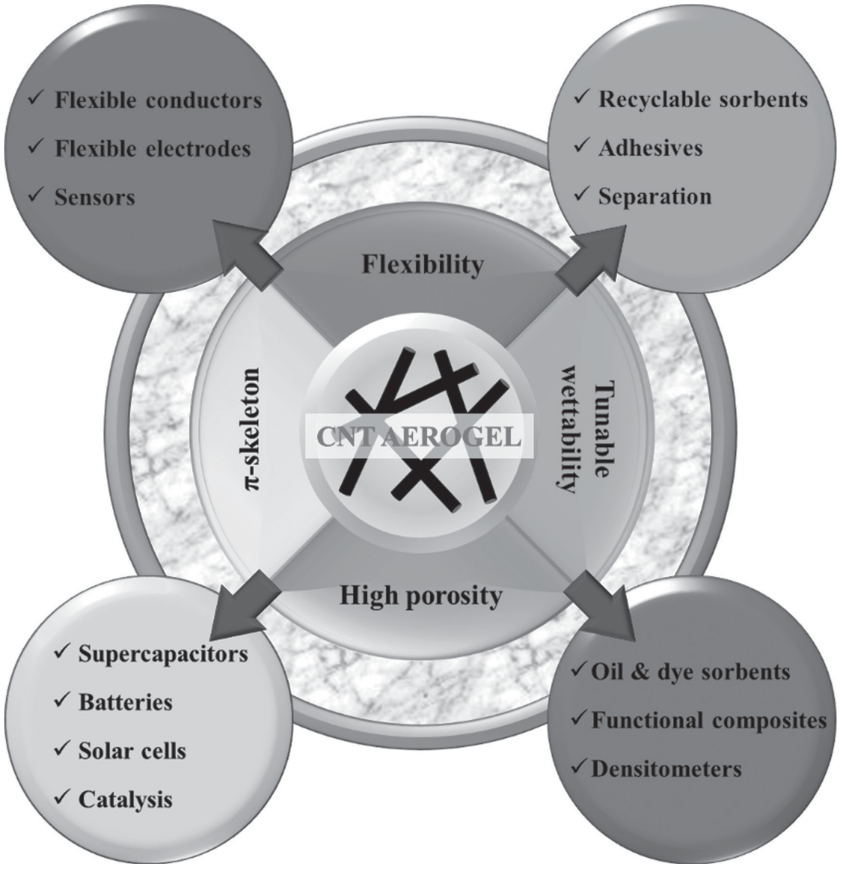

Figure 12. A summary of the potential properties and application fields of CNT-based aerogels.

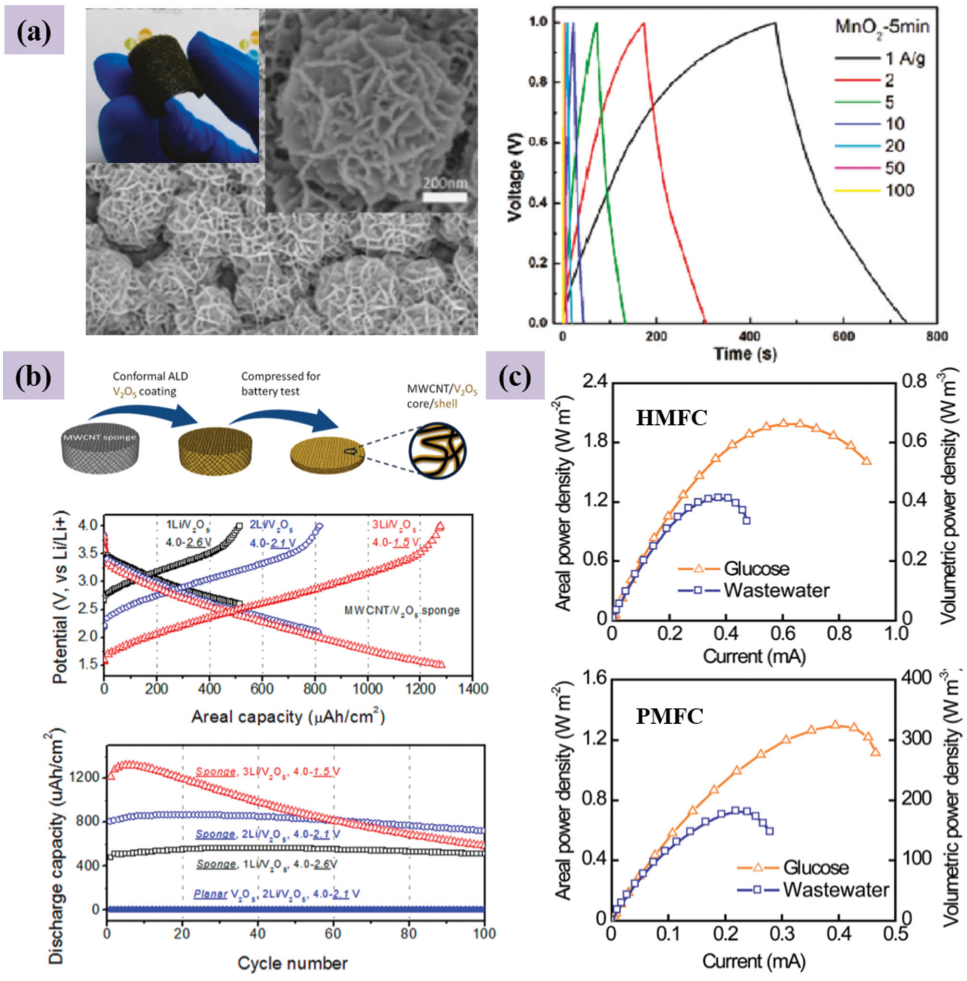

Figure 13. The applications of CNT-based aerogels in energy-related fields. a) High-performance nanostructured supercapacitors based on a MnO_2–CNT hybrid sponge electrode. Reproduced with permission.[121] Copyright 2011, American Chemical Society. b) MWCNT/V_2O_5 core/shell sponge for Li-ion cathodes. Reproduced with permission.[71] Copyright 2012, American Chemical Society. c) CNT-coated macroporous sponge for microbial fuel-cell electrodes. Reproduced with permission.[125] Copyright 2012, Royal Society of Chemistry.

design, the total capacitance can be significantly improved up to 1230 F g^{-1} at 1 mV s^{-1} (based on the mass of MnO_2) as a result of a combined double-layer capacitance from physical ion sorption and pseudocapacitance from the reversible redox reaction of metal oxides. In comparison, the MnO_2-loaded Pt electrode only gives rise to a capacitance of less than 200 F g^{-1} at the same scan rate. More importantly, the hybrid sponge can serve as both a current collector and an electrode material without a binder (which is always considered an electrochemically inert component), facilitating packaging and optimizing cell performance.

Compared with supercapacitors, the main obstacles for lithium-ion batteries (LIBs) are their low power density and short cycle life.[153] In this regard, high conductivity, large SSA, good mechanical stability are required for the electrode materials. Chen and co-workers[71] prepared MWCNT/V_2O_5 core/shell sponges via atomic layer deposition (ALD) of a thin, uniform layer of V_2O_5 on a CVD-grown MWCNT sponge, as shown in Figure 13b. The CNT sponge provided a conductive 3D network and hierarchical pores, facilitating fast electron and lithium-ion transfer and thus improving the power density. The high SSA of the sponge could also improve the energy density by increasing the number of accessible active sites. The V_2O_5 provided a high specific capacity (≈441 mAh g^{-1} with three Li de/intercalation per V_2O_5), and the ALD technique allowed the formation of a thin oxide layer closely contacting the CNT skeleton, which was beneficial for a high energy density and high power density, respectively. As a result, the composite sponge delivered a dramatically higher capacity (818 μAh cm^{-2}) than that of V_2O_5 film (1.8 μAh cm^{-2}) at a 1C rate. Additionally, the hybrid sponge achieved a high capacity (155 μAh cm^{-2}) and power density (21.7 mW cm^{-2}) even at a 50C rate. Compared with V_2O_5, silicon shows a much higher theoretical capacity (≈4200 mAh g^{-1}) with a fully lithiated composition of $Li_{4.4}Si$. However, the large volume change of Si during charge/discharge cycling leads to a poor cycle life. In this regard, Hu and co-workers deposited Si on CVD-grown CNT sponges via a CVD process. The CNT sponge provided a highly conductive pathway and served as a mechanically flexible support to accommodate the volume change of the loaded silicon. The resultant silicon–CNT

coaxial sponge anode exhibited a specific capacity as high as 2800 mAh g^{-1} with a cutoff of 0.05–1.0 V, and an excellent cycling performance without any obvious capacity fading over 50 cycles.

CNT-based aerogels have also been proven to be amazing electrode materials in bio-electrochemical systems.[125,154] As demonstrated by Xie and co-workers,[125] CNT-coated macroporous polyurethane sponges have shown the highest performance at that time when used as an electrode for microbial fuel cells (MFCs), with an areal power density of 1.24 W m^{-2} for a batch-fed H-shaped MFC (HMFC) and a maximum volumetric power density of 128 W m^{-3} for a continuously fed plate-shaped MFC (PMFC) in domestic wastewater treatment (Figure 13c). This is due to the combination of a continuous 3D conductive path throughout the sponge surface, appropriate pore sizes, and excellent mechanical properties of the hybrid sponge. It should be noted that the sponge form is very important. For comparison, when used as an MFC anode, the maximum current density of the CNT textile is ca. 32.4% lower than that of a CNT sponge under the same conditions.

4.2.2. Catalysis

CNT-based aerogels are promising for catalysis, serving as either scaffolds or as the catalysts themselves. A large SSA provides numerous active sites for reaction or loading, a tunable PSD facilitates mass transfer or shape-selective catalysis, high conductivity triggers fast reaction kinetics (especially for electrochemical catalysis), and high stability (chemical and mechanical) will guarantee long shelf life and cycle life.

The rational use of CNT-based aerogels as supports to load catalytic matter can create high-performance catalysts.[72,108,110,116,127] This is achieved by fully exposing the active catalysts and imparting a high conductivity to system for fast electron transfer. For example, photocatalytic decomposition of rhodamine B (RhB) has been achieved using a CNT/CdS nanoparticle sponge,[72] which utilized both the molecule adsorption ability of large-SSA CNT sponges and the photocatalytic activity of CdS nanoparticles. Intriguingly, since the internal CdS nanoparticles are protected during the reaction, after use, the sponge can be facilely regenerated by stripping off the surface part. In another work,[127] Pt nanoparticles (10 wt%, average size ≈5 nm) decorated a highly conductive MWCNT/chitosan (CHI) monolith, which was prepared by an ISISA method. The microchanelled structure enabled facile mass transport in catalyzing the methanol oxidation reaction, and the large SSA allowed Pt nanoparticles to be fully exposed to the reactants. Most importantly, unlike traditional catalysts where the reaction only occurs at the external surface, the aerogel-supported catalyst allowed a "bulk phase" catalysis throughout the gel network because of its porous structure. In this way, the catalytical current density linearly increases with increasing catalyst mass up to 10 mg (**Figure 14**a), which greatly improves the space utilization efficiency. CNT-based aerogels supporting Pt or CuO catalysts have also been reported to catalyze the CO oxidation reaction.[110,116]

Scientists have also found that surface-modified or doped CNTs themselves can be used as catalysts.[155,156] Therefore, CNT-based aerogels with an appropriate design can be directly employed as catalysts without loading metals. Recently, we demonstrated the preparation of nitrogen-doped CNT aerogels using an "erasable" promoter-assisted hydrothermal reaction coupled with pyrolysis.[126] It is known that nitrogen doping can induce local charge redistribution and thus "activate" the catalytical ability of inert CNTs.[156] The resultant highly conductive and high-SSA aerogels showed fascinating performances in oxygen reduction reaction (ORR) catalysis, with a positive onset potential (–0.055 V versus Ag/AgCl), high current density (higher than 20 wt% Pt/C at potentials lower than -0.4 V versus Ag/AgCl), and a dominant four-electron pathway (Figure 14b). The possible roles of trace metal residues (e.g., Fe, Mn) were excluded by contrast experiments and ion-poisoning experiments. The current density being higher than that of conventional N-CNT catalysts[157,158] suggests more active sites are present in N-CNT aerogels. In addition, theoretically, the monolithic aerogel itself can serve as a free-standing electrode without any binder, which would benefit practical applications.

One concern about CNT-based metal-free catalysts is that whether or not they are truly metal-free, as metals may be introduced during the growth or post-treatment processes. Highly sensitive characterization methods such as ICP-MS should be used to check for metal residues. However, in

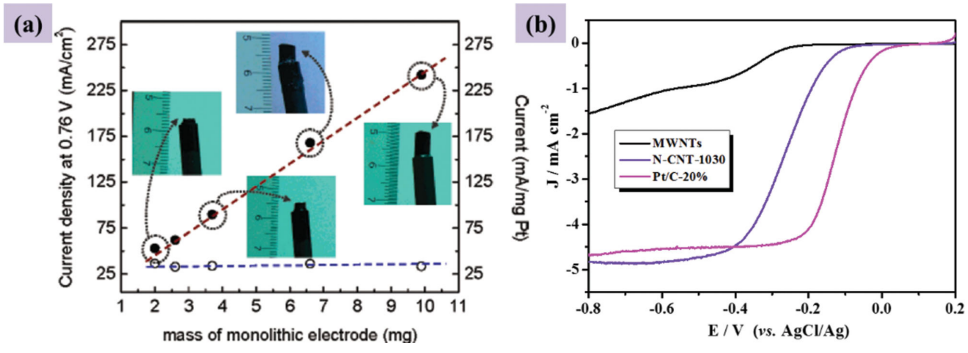

Figure 14. Examples of CNT-based aerogels for catalysis. a) Macroporous 3D MWCNT assemblies decorated with Pt nanoparticles for methanol oxidation catalysis. b) LSV curves of N-doped CNT aerogels in ORR catalysis. Reproduced with permission.[126,127] Copyright 2007, American Chemical Society.

pursuit of high catalytic performance and low production cost, the direct use of as-prepared metal-containing CNTs as catalysts might be better if the amount and type of metal residues were reproducible.

4.2.3. Water Treatment

CNT-based aerogels not only have a superior adsorption capacity towards organic solvents, oils, and dyestuffs due to the common features of aerogels (e.g., low density, hierarchical pores), but also show great potential for recycling usage and capacitive deionization (CDI) applications due to the intrinsic properties of CNTs (high thermal stability, excellent mechanical properties, and high conductivity).

Gui et al. reported CVD-grown CNT sponges exhibiting an oil uptake capacity of about 80–180 times their own weight.[55] In addition, the CVD process endowed the sponges with superhydrophobicity (contact angle ≈ 156°) and excellent mechanical properties, which facilitated their use in oil/water mixtures and regeneration by simple squeezing (**Figure 15**a).[55,159] Superhydrophobic CNT/graphene foam (density ≈ 7 mg cm^{-3}) has also showed a high sorption capacity of about 80–130 g g^{-1}.[67] A lower density can trigger a higher sorption capacity for liquids because of the enlarged accommodation space inside the aerogel. As shown by Sun and co-workers,[117] the ultra-flyweight CNT/graphene aerogel (0.16 mg cm^{-3}) exhibited a striking oil sorption capacity of up to 743 g g^{-1} for CCl_4. Additionally, thanks to the large average pore size (≈123 nm), the aerogel had an ultrafast adsorption rate for toluene at 68.8 g per gram of aerogel per second.

Dyestuffs are another type of pollutant in water which always possess aromatic rings. Hence, they should be easily captured by large-SSA aerogels via π–π interactions. It was reported that CNT sponges showed high filtration capacities towards RhB (up to 3.3 L g^{-1} for RhB at 0.02 mM).[160] Recently, Zhang and co-workers[112] showed an interesting dendrimer-linked renewable CNT aerogel. Taking advantage of pH-sensitive ionic crosslinkages between carboxylic acid groups on oxidized CNTs and amino groups on poly-(amido amine) (PAMAM), after the adsorption of methylene blue (MB), the hybrid aerogel could be regenerated via a following desorption and reversible sol–gel transition process, as shown in Figure 15c.

Capacitive deionization is a promising method for brackish water desalination by trapping salts via the electrical double layer. Based on this mechanism, electrode materials with a large SSA, high electrical conductivity, and appropriate PSD are highly desired, so as to achieve large electrical double-layer capacitance and fast adsorption/desorption.

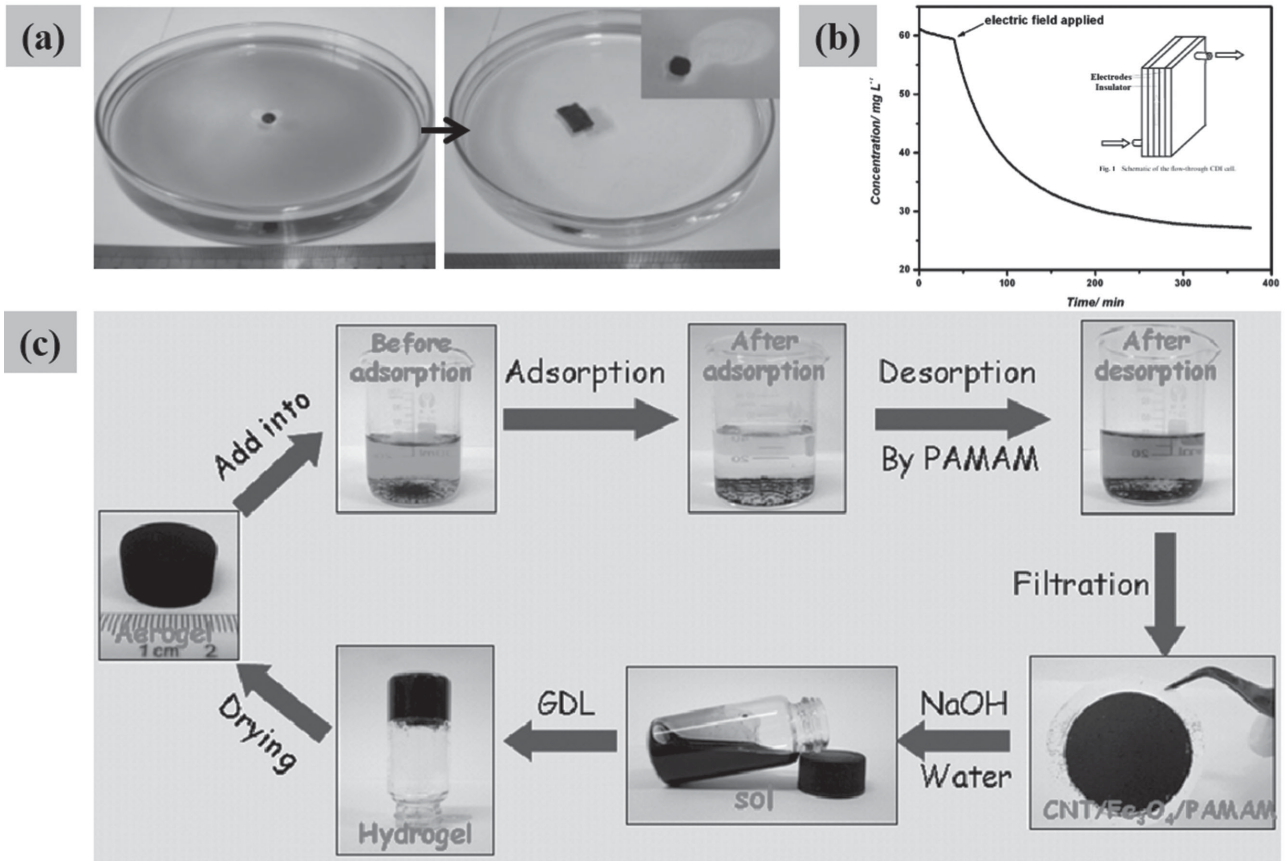

Figure 15. Demonstration of the use of CNT-based aerogels for oil uptake, capacitive deionization, and dye sorption. a) Adsorption of vegetable oil (dyed blue) by a piece of CNT sponge. Reproduced with permission.[55] Copyright 2010, Wiley-VCH. b) The desalination curve for CNT sponges in a CDI cell. Inset is the schematic of a flow-through CDI cell. Reproduced with permission.[162] Copyright 2011, Royal Society of Chemistry. c) The demonstration of recycling dendrimer-linked CNT aerogels for methylene blue sorption. Reproduced with permission.[112] Copyright 2014, Royal Society of Chemistry.

Considering this, CNT aerogels are one of the most promising candidates for capacitive deionization (CDI) applications.[114,161,162] For example, Wang and co-workers[161] assembled a flow-through CDI cell using CVD-grown CNT sponges with SSAs of about 60–80 $m^2 g^{-1}$ (Figure 15b). The device showed a maximum electrosorption capacity of 40.1 mg g^{-1} (derived from the Langmuir model) towards NaCl at 1.2 V bias voltage; much higher than most other materials. This result not only comes from the monolithic structure (without the requirement of adhesives, which may block the pores and reduce the conductivity), but also from its high conductivity and appropriate PSD (meso- and macropores) for efficient electron and mass transfer. In a similar work, Sui and co-workers[114] showed that a graphene-MWCNT aerogel can achieve an incredible removal capacity of 633.3 mg g^{-1} at 1.0 V bias voltage 35 000 mg L^{-1} NaCl aqueous solution. In this case, the experimental data was fitted well by a Freundlich isotherm rather than the Langmuir isotherm. They claim that this huge sorption capacity was the combination of hierarchical pores, introduced functional groups, high conductivity (7.5 S m^{-1}) due to the hybrid structure of graphene and CNTs, and the large SSA (435 $m^2 g^{-1}$).

It should be noted, however, that other aerogels, e.g., graphene aerogels and carbon fiber aerogels,[149,163] can also be applied for water treatment and show even better performance than CNT-based aerogels in some cases. The challenges and opportunities for CNT aerogels lie in the development of fabrication methods towards lighter aerogels with controlled CNT structures for selective sorption.

4.2.4. Other Applications

Besides the above applications, CNT-based aerogels can also be applied in other fields including adhesives,[164] sensors,[66,68,70,117,120,130,165,167] optics,[111,121] electrochemical detection,[166] tissue engineering,[167] artificial muscles,[168] and energy absorption.[169]

Inspired by gecko feet, Qu and co-workers[164] synthesized a CNT array with a straight body section and a curly, entangled top (**Figure 16**a). It showed excellent normal adhesive forces (10–20 N cm^{-2}) and a high shear adhesion force (up to 100 N cm^{-2}), which mimics gecko feet in binding strongly along the shear direction but with easy lifting along normal the direction. The adhesion force originated from the van der Waals force between the CNTs and the substrate. The enhanced shear adhesion force was attributed to an enlarged contact area and more intimate contact induced by shear alignment of the entangled random CNTs at the top section when the CNT array a shear force was applied.

Combining compressibility and high conductivity, both nitrogen-doped CNT sponges obtained from CVD growth[66] and CNT/graphene aerogels acquired from wet chemistry methods[117] show potential as pressure sensors (Figure 16b,c). When the aerogel is compressed, the conductivity is considerably improved because of increased inter-tube contacting points (i.e., conducting paths), and vice versa. To enhance the mechanical properties (e.g., flexibility, elasticity) of pure CNT aerogels, polymers (e.g., polydimethylsiloxane, epoxy resin) can be introduced by infiltration.[70,165] CNT aerogels also show high sensitivity towards chemicals in water or gases, which allows their use in electrochemical and gas sensing.[68,130] Compared with microscopic sensors, the macroscopic aerogel affords an easy device assembly procedure and large signal change, facilitating practical production and monitoring.

In addition to this, the infrared fluorescence of SWCNTs has allowed scientists to investigate optics-related properties of SWCNT-based aerogels prepared by noncovalent crosslinking.[111,121] To expand the use of this property, a

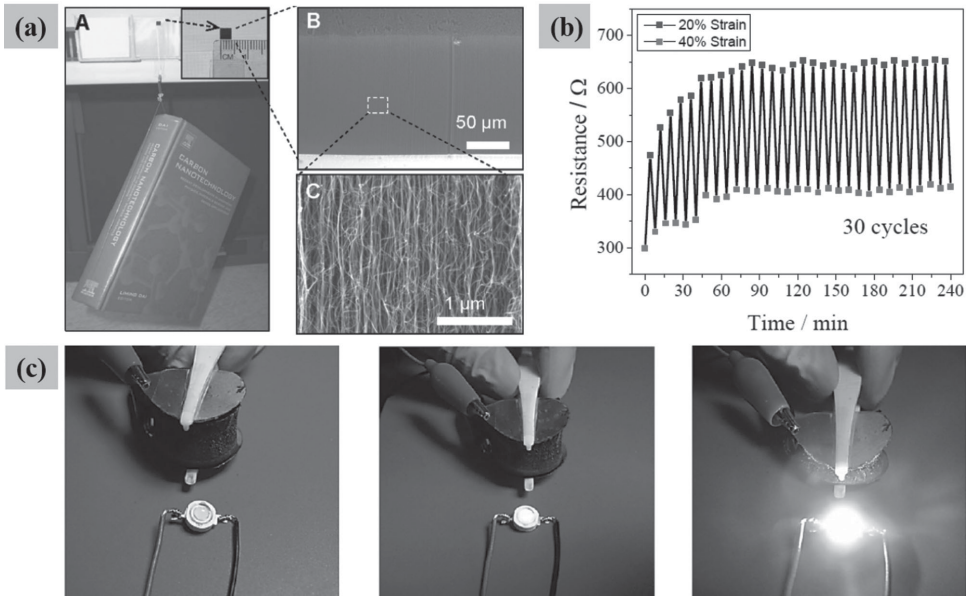

Figure 16. a) CNT vertical arrays as adhesives. Reproduced with permission.[165] Copyright 2011, American Association for the Advancement of Science. The potential use of b) N-doped CNT aerogels. Reproduced with permission.[66] Copyright 2013, American Chemical Society.c) ultralight CNT/graphene composite aerogels as pressure sensors. Reproduced with permission.[117] Copyright 2013, Wiley-VCH.

modified SWCNT aerogel may be used in drug-delivery systems for simultaneous drug release (the drug can be gradually released or released in a controlled way from the pores of the gel matrix) and in-situ imaging. Combining the high modulus of CNT arrays and large strain of CNT sponges, CNT sponge-array tandem arrays were created by CVD to serve as efficient energy-absorption materials.[169] Additionally, although with some toxicity concerns about CNTs, MWCNT/chitosan scaffolds were proven to be biocompatible and biodegradable supports both in vitro and in vivo. The scaffold could adsorb recombinant human bone morphogenetic protein-2 (rhBMP-2) and thus promote ectopic bone formation at muscle tissue.[167]

4.2.5. Aerogels as Platforms for the Production of Other Macroscopic Assemblies

3D CNT-based aerogels can serve as a platform for producing other CNT-based, multiscaled, macroscopic assemblies. This is an interesting and unique application for CNT monoliths, which has not been applied to other aerogel systems based on graphene, carbon, metals, or other materials. In this field, most work starts with pure CNT aerogels, especially for the production of 1D CNT fibers and 2D CNT films.

One-dimensional CNT fibers can be drawn from either CNT arrays or CNT aerogels.[42–44,170] For example, Windle's group showed that 1D CNT fibers can be in-situ spun from CNT aerogels growing in a hot furnace using a rotating spindle (**Figure 17**a).[43] In this way, the number of CNT walls can be modulated by the reaction conditions and corresponding desired CNT fibers can be continuously produced. The same group[44] further showed that by introducing an on-line densification process assisted by an acetone vapor stream, the CNT fiber drawn from the aerogels achieved an ultrahigh strength (broken strength, approaching 10 N tex^{-1}, where tex is the linear density in g km^{-1}) and stiffness (axial elastic modulus, approaching 400 N tex^{-1}), much higher than that of commercial polymer fibers and other CNT fibers.

Two-dimensional CNT sheets and films can also be obtained from CNT aerogels or vertical arrays.[43,47,168] Via a simple modification of the former, aligned CNT films can also be in-situ acquired by the same technique as for the

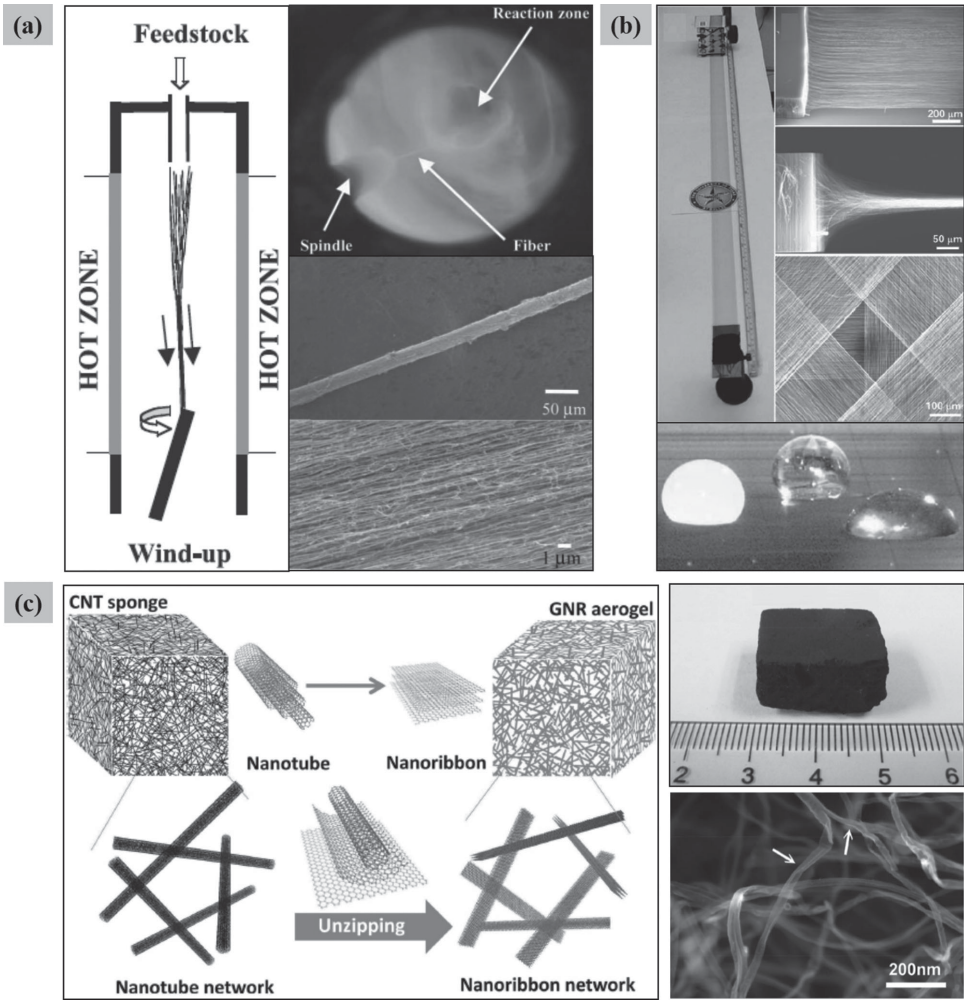

Figure 17. Demonstration of CNT aerogels as the platform for producing a) 1D CNT fibers (reproduced with permission.[43] Copyright 2004, American Association for the Advancement of Science), b) 2D CNT sheets (reproduced with permission.[47] Copyright 2005, American Association for the Advancement of Science), c) 3D graphene nanoribbon (GNR) aerogels. Reproduced with permission.[171] Copyright 2014, Wiley-VCH.

gas-phase production of CNT fibers.[43] In another work, 5 cm-wide, meter-long, transparent sheets were drawn from a CNT vertical array (Figure 17b).[47] However, up to now, there has been no report of 1D or 2D CNT macroscopic assemblies acquired from as-prepared 3D isotropic CNT aerogels. The difficulties lie in two aspects. Individual CNTs in aerogels (especially those derived from wet chemistry) are too short to gain enough inter-tube van der Waals interactions, thus making it impossible to create continuous fibers or films. Secondly, the random nature of isotropic aerogels may place a difficulty on untangling the individual CNTs, and thereby inhibiting the drawing process.

CNT-based aerogels can also be converted to other types of 3D assemblies. As mentioned in Sections 2 and 3, after decoration with Pt nanoparticles,[127] CdS nanoparticles,[72] or oxides (SiO_2, SnO_2, or TiO_2),[108] the resultant composite aerogels can be tailored for specific applications such as photocatalysis and methanol oxidation catalysis. Cao's group recently showed the conversion of CNT sponges to a graphene nanoribbon (GNR) aerogel by in-situ chemical unzipping of CNTs with $KMnO_4$ in concentrated H_2SO_4 without sonication (Figure 17c).[171] Due to the excellent mechanical properties of the original CNT sponges derived from long and entangled individual CNTs, the resultant graphene aerogel maintains the shape and original network structure of the CNT sponge. Besides the traditional bottom-up approach, this kind of "macroscopic conversion" method provides a new strategy for synthesizing 3D assemblies.

5. Conclusion and Outlook

In the last twenty years, numerous scientists have devoted themselves to the study of CNTs, ranging from studies of basic properties, growth mechanisms, chirality enrichment, macroscopic assembly preparation, to practical applications. The understanding of the fundamental properties and growth mechanisms of CNTs has been considerably improved, the production costs to make CNTs are continuously reduced with profound progress in preparation techniques, and CNTs have truly entered practical applications including batteries and additives. However, until now, some very fundamental issues still puzzle scientists. One of the greatest challenges is to extend the individual properties of CNTs to their macroscopic assemblies. Together with the relative high cost (especially for SWCNTs), a low performance-to-cost ratio will be the major obstacle for the wide commercialization of CNT-based products.

In more recent years, encouraging results have shown that, when CNTs appear in a new form, i.e., CNT-based 3D monoliths (aerogels), things are different. Combining the features of aerogels (hierarchical open pores, low density, interconnected networks, a monolithic architecture) and individual CNTs (exceptional mechanical properties, high electrical/thermal conductivity, high stability, large specific surface area), they exhibit remarkable performance and multiple functions for diverse applications. Therefore, CNT-based 3D monoliths may be a breakthrough for fully exploiting the properties of individual CNTs and thereby accelerating the commercialization step of CNT-based products.

In this article, we have provided a comprehensive review of CNT-based 3D monoliths. Preparation strategies can be divided into two main classes: direct CVD growth, and wet chemistry (either a sol–gel process or direct freeze drying). The former method can create high quality aerogels constructed from long individual CNTs in one step, suitable for applications requiring exceptional electrical and mechanical properties. The latter enjoys more flexibility in both precursor selection (e.g., different types of CNTs, various additives) and synthetic approaches, promising for tailoring desirable functions of materials. Diverse potential applications (e.g., energy storage, catalysis, water treatment, pressure/gas sensors, energy absorption) have also been reviewed, confirming that the unique combination of CNTs and aerogels has enormous practical value. Directed by the main application fields and synthetic methods described here, one may get a clear picture about how to design these materials using appropriate precursors and strategies to achieve a high performance at an acceptable cost. Although we are trying to cover all preparation methods and applications of CNT-based 3D monoliths, there are many excellent works which may have been omitted unintentionally.

By carefully selecting synthetic methods, designing appropriate crosslinking forces, and introducing functional ingredients, CNT-based 3D monoliths with superior properties can be readily produced. Currently, however, the field of CNT-based 3D monoliths is far from mature: joint efforts from researchers of different backgrounds are needed. Firstly, cutting down the cost of CNT precursors by production technique development is required for their commercialization and competition with other materials (e.g., graphene-based aerogels, carbon aerogels). Secondly, combining the advantages of both dry chemistry and wet chemistry for aerogel preparation is highly desired. In this way, one can facilely investigate correlations between material performance and the precursors (e.g., different CNTs, other additives) to find general rules for efficient design and desired functions, by the smart introduction of extra ingredients (molecules or heteroatoms), and achieve optimal performance from high-quality individual CNTs. Thirdly, the tubular geometry and structural diversity of CNTs (e.g., the number of walls, chiralities, diameters), which make CNTs distinct from other materials, have not been well studied. Based on these features, CNTs can display structure-dependent properties (electrical conductivity, optical absorption, space-confined reactions, etc.), which may render CNT aerogels as high-performance materials for a wide range of applications including batteries, electronic devices, optics, and special reaction containers. It should be noted that the investigation of these properties also calls for substantial progress in the controllable synthesis of CNTs with accurate and desired structures. Finally, elegant synthetic approaches and relevant applications should be learned from other fields and other materials, since the field itself is a subject that requires interdisciplinary knowledge from materials science, engineering, chemistry, physics, information science, biology, and so on.

Therefore, both great challenges and enormous opportunities exist in this young field. We believe that with joint efforts from researchers across multiple disciplines, the

understanding of CNT-based 3D monoliths can be greatly improved, and both the preparation and application territory can be largely increased. In the future, this new material will surely make a big change to the CNT and materials industries.

Acknowledgements

This work was supported by the NSFC (21233001, 21129001, 51272006, 51121091 and 51432002) and MOST (2011CB932601). The photo in the right-hand corner of the Table of Contents picture is reproduced with permission.[121] Copyright 2011, American Chemical Society.

[1] S. Iijima, *Nature* **1991**, *354*, 56.
[2] P. M. Ajayan, *Chem. Rev.* **1999**, *99*, 1787.
[3] E. T. Thostenson, Z. F. Ren, T. W. Chou, *Compos. Sci. Technol.* **2001**, *61*, 1899.
[4] R. H. Baughman, A. A. Zakhidov, W. A. de Heer, *Science* **2002**, *297*, 787.
[5] J. M. Schnorr, T. M. Swager, *Chem. Mater.* **2011**, *23*, 646.
[6] M. F. L. De Volder, S. H. Tawfick, R. H. Baughman, A. J. Hart, *Science* **2013**, *339*, 535.
[7] L. Mleczko, G. Lolli, *Angew. Chem. Int. Ed.* **2013**, *52*, 9372.
[8] Y. B. Chen, J. Zhang, *Acc. Chem. Res.* **2014**, *47*, 2273.
[9] A. G. Rinzler, J. H. Hafner, P. Nikolaev, L. Lou, S. G. Kim, D. Tomanek, P. Nordlander, D. T. Colbert, R. E. Smalley, *Science* **1995**, *269*, 1550.
[10] H. J. Dai, J. H. Hafner, A. G. Rinzler, D. T. Colbert, R. E. Smalley, *Nature* **1996**, *384*, 147.
[11] S. J. Tans, A. R. M. Verschueren, C. Dekker, *Nature* **1998**, *393*, 49.
[12] P. Kim, C. M. Lieber, *Science* **1999**, *286*, 2148.
[13] J. Kong, N. R. Franklin, C. W. Zhou, M. G. Chapline, S. Peng, K. J. Cho, H. J. Dai, *Science* **2000**, *287*, 622.
[14] H. Qian, E. S. Greenhalgh, M. S. P. Shaffer, A. Bismarck, *J. Mater. Chem.* **2010**, *20*, 4751.
[15] L. Liu, W. Ma, Z. Zhang, *Small* **2011**, *7*, 1504.
[16] M. Pasta, F. La Mantia, L. Hu, H. Deshazer, Y. Cui, *Nano Res.* **2010**, *3*, 452.
[17] Y. Peng, Z. Chen, J. Wen, Q. Xiao, D. Weng, S. He, H. Geng, Y. Lu, *Nano Res.* **2011**, *4*, 216.
[18] S. X. Qiu Longbin, Yang Zhibin, Guo Wenhan, Peng Huisheng, *Acta Chim. Sinica* **2012**, *70*, 1523.
[19] J. Wu, Y. Xue, X. Yan, W. Yan, Q. Cheng, Y. Xie, *Nano Res.* **2012**, *5*, 521.
[20] Z. J. Zhang Yingying, *Acta Chim. Sinica* **2012**, *70*, 2293.
[21] M. Bailey, J. Heddleston, J. Davis, J. Staymates, A. Hight Walker, *Nano Res.* **2014**, *7*, 390.
[22] N. Hüsing, U. Schubert, *Angew. Chem. Int. Ed.* **1998**, *37*, 22.
[23] D. R. Rolison, B. Dunn, *J. Mater. Chem.* **2001**, *11*, 963.
[24] A. C. Pierre, G. M. Pajonk, *Chem. Rev.* **2002**, *102*, 4243.
[25] J. Lee, J. Kim, T. Hyeon, *Adv. Mater.* **2006**, *18*, 2073.
[26] N. Leventis, *Acc. Chem. Res.* **2007**, *40*, 874.
[27] B. C. Tappan, S. A. Steiner, E. P. Luther, *Angew. Chem. Int. Ed.* **2010**, *49*, 4544.
[28] J. Biener, M. Stadermann, M. Suss, M. A. Worsley, M. M. Biener, K. A. Rose, T. F. Baumann, *Energy Environ. Sci.* **2011**, *4*, 656.
[29] S. Nardecchia, D. Carriazo, M. L. Ferrer, M. C. Gutierrez, F. del Monte, *Chem. Soc. Rev.* **2013**, *42*, 794.
[30] F. Yang, X. Wang, D. Zhang, J. Yang, LuoDa, Z. Xu, J. Wei, J.-Q. Wang, Z. Xu, F. Peng, X. Li, R. Li, Y. Li, M. Li, X. Bai, F. Ding, Y. Li, *Nature* **2014**, *510*, 522.
[31] J. Prasek, J. Drbohlavova, J. Chomoucka, J. Hubalek, O. Jasek, V. Adam, R. Kizek, *J. Mater. Chem.* **2011**, *21*, 15872.
[32] M. S. Dresselhaus, G. Dresselhaus, R. Saito, A. Jorio, *Phys. Rep.* **2005**, *409*, 47.
[33] Y. Chen, Y. Zhang, Y. Hu, L. Kang, S. Zhang, H. Xie, D. Liu, Q. Zhao, Q. Li, J. Zhang, *Adv. Mater.* **2014**, *26*, 5898.
[34] P.-X. Hou, C. Liu, H.-M. Cheng, *Carbon* **2008**, *46*, 2003.
[35] A. F. Ismail, P. S. Goh, J. C. Tee, S. M. Sanip, M. Aziz, *Nano* **2008**, *03*, 127.
[36] I. Kruusenberg, N. Alexeyeva, K. Tammeveski, J. Kozlova, L. Matisen, V. Sammelselg, J. Solla-Gullon, J. M. Feliu, *Carbon* **2011**, *49*, 4031.
[37] Y. H. Yan, M. B. Chan-Park, Q. Zhang, *Small* **2007**, *3*, 24.
[38] B. Vigolo, A. Penicaud, C. Coulon, C. Sauder, R. Pailler, C. Journet, P. Bernier, P. Poulin, *Science* **2000**, *290*, 1331.
[39] L. M. Ericson, H. Fan, H. Q. Peng, V. A. Davis, W. Zhou, J. Sulpizio, Y. H. Wang, R. Booker, J. Vavro, C. Guthy, A. N. G. Parra-Vasquez, M. J. Kim, S. Ramesh, R. K. Saini, C. Kittrell, G. Lavin, H. Schmidt, W. W. Adams, W. E. Billups, M. Pasquali, W. F. Hwang, R. H. Hauge, J. E. Fischer, R. E. Smalley, *Science* **2004**, *305*, 1447.
[40] V. A. Davis, A. N. G. Parra-Vasquez, M. J. Green, P. K. Rai, N. Behabtu, V. Prieto, R. D. Booker, J. Schmidt, E. Kesselman, W. Zhou, H. Fan, W. W. Adams, R. H. Hauge, J. E. Fischer, Y. Cohen, Y. Talmon, R. E. Smalley, M. Pasquali, *Nat. Nanotechnol.* **2009**, *4*, 830.
[41] N. Behabtu, C. C. Young, D. E. Tsentalovich, O. Kleinerman, X. Wang, A. W. K. Ma, E. A. Bengio, R. F. ter Waarbeek, J. J. de Jong, R. E. Hoogerwerf, S. B. Fairchild, J. B. Ferguson, B. Maruyama, J. Kono, Y. Talmon, Y. Cohen, M. J. Otto, M. Pasquali, *Science* **2013**, *339*, 182.
[42] K. L. Jiang, Q. Q. Li, S. S. Fan, *Nature* **2002**, *419*, 801.
[43] Y. L. Li, I. A. Kinloch, A. H. Windle, *Science* **2004**, *304*, 276.
[44] K. Koziol, J. Vilatela, A. Moisala, M. Motta, P. Cunniff, M. Sennett, A. Windle, *Science* **2007**, *318*, 1892.
[45] N. Behabtu, M. J. Green, M. Pasquali, *Nano Today* **2008**, *3*, 24.
[46] W. Lu, M. Zu, J.-H. Byun, B.-S. Kim, T.-W. Chou, *Adv. Mater.* **2012**, *24*, 1805.
[47] M. Zhang, S. L. Fang, A. A. Zakhidov, S. B. Lee, A. E. Aliev, C. D. Williams, K. R. Atkinson, R. H. Baughman, *Science* **2005**, *309*, 1215.
[48] L. Xiao, Z. Chen, C. Feng, L. Liu, Z. Q. Bai, Y. Wang, L. Qian, Y. Y. Zhang, Q. Q. Li, K. L. Jiang, S. S. Fan, *Nano Lett.* **2008**, *8*, 4539.
[49] Z. Shi, W. B. Zhang, F. Zhang, X. Liu, D. Wang, J. Jin, L. Jiang, *Adv. Mater.* **2013**, *25*, 2422.
[50] L. Song, L. Ci, L. Lv, Z. P. Zhou, X. Q. Yan, D. F. Liu, H. J. Yuan, Y. Gao, J. X. Wang, L. F. Liu, X. W. Zhao, Z. X. Zhang, X. Y. Dou, W. Y. Zhou, G. Wang, C. Y. Wang, S. S. Xie, *Adv. Mater.* **2004**, *16*, 1529.
[51] W. J. Ma, L. Song, R. Yang, T. H. Zhang, Y. C. Zhao, L. F. Sun, Y. Ren, D. F. Liu, L. F. Liu, J. Shen, Z. X. Zhang, Y. J. Xiang, W. Y. Zhou, S. S. Xie, *Nano Lett.* **2007**, *7*, 2307.
[52] J. T. Di, D. M. Hu, H. Y. Chen, Z. Z. Yong, M. H. Chen, Z. H. Feng, Y. T. Zhu, Q. W. Li, *ACS Nano* **2012**, *6*, 5457.
[53] M. B. Bryning, D. E. Milkie, M. F. Islam, L. A. Hough, J. M. Kikkawa, A. G. Yodh, *Adv. Mater.* **2007**, *19*, 661.
[54] M. De Volder, S. H. Tawfick, S. J. Park, D. Copic, Z. Z. Zhao, W. Lu, A. J. Hart, *Adv. Mater.* **2010**, *22*, 4384.
[55] X. Gui, J. Wei, K. Wang, A. Cao, H. Zhu, Y. Jia, Q. Shu, D. Wu, *Adv. Mater.* **2010**, *22*, 617.
[56] A. Tabet-Aoul, M. Mohamedi, *J. Mater. Chem.* **2012**, *22*, 2491.
[57] W. D. Cho, M. Schulz, V. Shanot, *Carbon* **2014**, *72*, 264.
[58] L. L. Jiang, Z. J. Fan, *Nanoscale* **2014**, *6*, 1922.

[59] Z. Q. Niu, L. L. Liu, L. Zhang, X. D. Chen, *Small* **2014**, *10*, 3434.
[60] M. Xu, D. N. Futaba, M. Yumura, K. Hata, *ACS Nano* **2012**, *6*, 5837.
[61] W. Z. Li, S. S. Xie, L. X. Qian, B. H. Chang, B. S. Zou, W. Y. Zhou, R. A. Zhao, G. Wang, *Science* **1996**, *274*, 1701.
[62] K. Hata, D. N. Futaba, K. Mizuno, T. Namai, M. Yumura, S. Iijima, *Science* **2004**, *306*, 1362.
[63] Y. H. Yun, V. Shanov, Y. Tu, S. Subramaniam, M. J. Schulz, *J. Phys. Chem. B* **2006**, *110*, 23920.
[64] L. X. Zheng, X. F. Zhang, Q. W. Li, S. B. Chikkannanavar, Y. Li, Y. H. Zhao, X. Z. Liao, Q. X. Jia, S. K. Doorn, D. E. Peterson, Y. T. Zhu, *Adv. Mater.* **2007**, *19*, 2567.
[65] D. P. Hashim, N. T. Narayanan, J. M. Romo-Herrera, D. A. Cullen, M. G. Hahm, P. Lezzi, J. R. Suttle, D. Kelkhoff, E. Munoz-Sandoval, S. Ganguli, *Sci. Rep.* **2012**, *2*, 363.
[66] C. Shan, W. Zhao, X. L. Lu, D. J. O'Brien, Y. Li, Z. Cao, A. L. Elias, R. Cruz-Silva, M. Terrones, B. Wei, *Nano Lett.* **2013**, *13*, 5514.
[67] X. Dong, J. Chen, Y. Ma, J. Wang, M. B. Chan-Park, X. Liu, L. Wang, W. Huang, P. Chen, *Chem. Commun.* **2012**, *48*, 10660.
[68] X. C. Dong, Y. W. Ma, G. Y. Zhu, Y. X. Huang, J. Wang, M. B. Chan-Park, L. H. Wang, W. Huang, P. Chen, *J. Mater. Chem.* **2012**, *22*, 17044.
[69] W. Wang, S. R. Guo, M. Penchev, I. Ruiz, K. N. Bozhilov, D. Yan, M. Ozkan, C. S. Ozkan, *Nano Energy* **2013**, *2*, 294.
[70] X. C. Gui, A. Y. Cao, J. Q. Wei, H. B. Li, Y. Jia, Z. Li, L. L. Fan, K. L. Wang, H. W. Zhu, D. H. Wu, *ACS Nano* **2010**, *4*, 2320.
[71] X. Y. Chen, H. L. Zhu, Y. C. Chen, Y. Y. Shang, A. Y. Cao, L. B. Hu, G. W. Rubloff, *ACS Nano* **2012**, *6*, 7948.
[72] H. B. Li, X. C. Gui, C. Y. Ji, P. X. Li, Z. Li, L. H. Zhang, E. Z. Shi, K. Zhu, J. Q. Wei, K. L. Wang, H. W. Zhu, D. H. Wu, A. Y. Cao, *Nano Res.* **2012**, *5*, 265.
[73] W. Wenseleers, Vlasov, II, E. Goovaerts, E. D. Obraztsova, A. S. Lobach, A. Bouwen, *Adv. Funct. Mater.* **2004**, *14*, 1105.
[74] V. Datsyuk, M. Kalyva, K. Papagelis, J. Parthenios, D. Tasis, A. Siokou, I. Kallitsis, C. Galiotis, *Carbon* **2008**, *46*, 833.
[75] M. J. Green, *Polym. Int.* **2010**, *59*, 1319.
[76] Y. Y. Huang, E. M. Terentjev, *Polymers* **2012**, *4*, 275.
[77] S. W. Kim, T. Kim, Y. S. Kim, H. S. Choi, H. J. Lim, S. J. Yang, C. R. Park, *Carbon* **2012**, *50*, 3.
[78] E. N. Primo, F. A. Gutierrez, G. L. Luque, P. R. Dalmasso, A. Gasnier, Y. Jalit, M. Moreno, M. V. Bracamonte, M. E. Rubio, M. L. Pedano, M. C. Rodriguez, N. F. Ferreyra, M. D. Rubianes, S. Bollo, G. A. Rivas, *Anal. Chim. Acta* **2013**, *805*, 19.
[79] R. Du, N. Zhang, H. Xu, N. N. Mao, W. J. Duan, J. Y. Wang, Q. C. Zhao, Z. F. Liu, J. Zhang, *Adv. Mater.* **2014**, DOI: 10.1002/adma.201403058.
[80] M. Antonietti, N. Fechler, T. P. Fellinger, *Chem. Mater.* **2014**, *26*, 196.
[81] L. A. Hough, M. F. Islam, B. Hammouda, A. G. Yodh, P. A. Heiney, *Nano Lett.* **2006**, *6*, 313.
[82] L. A. Hough, M. F. Islam, P. A. Janmey, A. G. Yodh, *Phys. Rev. Lett.* **2004**, *93*.
[83] S. N. Schiffres, K. H. Kim, L. Hu, A. J. H. McGaughey, M. F. Islam, J. A. Malen, *Adv. Funct. Mater.* **2012**, *22*, 5251.
[84] Z. Q. Tan, S. Ohara, M. Naito, H. Abe, *Adv. Mater.* **2011**, *23*, 4053.
[85] Y. Sabba, E. L. Thomas, *Macromolecules* **2004**, *37*, 6662.
[86] M. S. P. Shaffer, X. Fan, A. H. Windle, *Carbon* **1998**, *36*, 1603.
[87] N. I. Kovtyukhova, T. E. Mallouk, L. Pan, E. C. Dickey, *J. Am. Chem. Soc.* **2003**, *125*, 9761.
[88] Y. Xu, K. Sheng, C. Li, G. Shi, *ACS Nano* **2010**, *4*, 4324.
[89] Z. Y. Sui, X. T. Zhang, Y. Lei, Y. J. Luo, *Carbon* **2011**, *49*, 4314.
[90] J. Y. Luo, V. C. Tung, A. R. Koltonow, H. D. Jang, J. X. Huang, *J. Mater. Chem.* **2012**, *22*, 12993.
[91] T. Fukushima, A. Kosaka, Y. Ishimura, T. Yamamoto, T. Takigawa, N. Ishii, T. Aida, *Science* **2003**, *300*, 2072.
[92] T. Fukushima, T. Aida, *Chem.—Eur. J.* **2007**, *13*, 5048.
[93] R. Du, J. Wu, L. Chen, H. Huang, X. Zhang, J. Zhang, *Small* **2014**, *10*, 1387.
[94] M. K. Bayazit, L. S. Clarke, K. S. Coleman, N. Clarke, *J. Am. Chem. Soc.* **2010**, *132*, 15814.
[95] E. J. Cheng, Y. L. Li, Z. Q. Yang, Z. X. Deng, D. S. Liu, *Chem. Commun.* **2011**, *47*, 5545.
[96] S. Srinivasan, S. S. Babu, V. K. Praveen, A. Ajayaghosh, *Angew. Chem. Int. Ed.* **2008**, *47*, 5746.
[97] L. Lascialfari, C. Vinattieri, G. Ghini, L. Luconi, D. Berti, M. Mannini, C. Bianchini, A. Brandi, G. Giambastiani, S. Cicchi, *Soft Matter* **2011**, *7*, 10660.
[98] J. Chen, C. H. Xue, R. Ramasubramaniam, H. Y. Liu, *Carbon* **2006**, *44*, 2142.
[99] X. Tong, J. G. Zheng, Y. C. Lu, Z. F. Zhang, H. M. Cheng, *Mater. Lett.* **2007**, *61*, 1704.
[100] Z. M. Wang, Y. M. Chen, *Macromolecules* **2007**, *40*, 3402.
[101] S. Bhattacharyya, S. Guillott, H. Dabboue, J. F. Tranchant, J. P. Salvetat, *Biomacromolecules* **2008**, *9*, 505.
[102] A. Pal, B. S. Chhikara, A. Govindaraj, S. Bhattacharya, C. N. R. Rao, *J. Mater. Chem.* **2008**, *18*, 2593.
[103] M. Vaysse, M. K. Khan, P. Sundararajan, *Langmuir* **2009**, *25*, 7042.
[104] X. B. Zhang, C. L. Pint, M. H. Lee, B. E. Schubert, A. Jamshidi, K. Takei, H. Ko, A. Gillies, R. Bardhan, J. J. Urban, M. Wu, R. Fearing, A. Javey, *Nano Lett.* **2011**, *11*, 3239.
[105] S. Roy, A. Banerjee, *RSC Adv.* **2012**, *2*, 2105.
[106] K. H. Kim, Y. Oh, M. F. Islam, *Adv. Funct. Mater.* **2013**, *23*, 377.
[107] S. M. Jung, H. Y. Jung, M. S. Dresselhaus, Y. J. Jung, J. Kong, *Sci. Rep.* **2012**, *2*, 849.
[108] M. A. Worsley, S. O. Kucheyev, J. D. Kuntz, T. Y. Olson, T. Y. J. Han, A. V. Hamza, J. H. Satcher, T. F. Baumann, *Chem. Mater.* **2011**, *23*, 3054.
[109] R. R. Kohlmeyer, M. Lor, J. Deng, H. Liu, J. Chen, *Carbon* **2011**, *49*, 2352.
[110] S. H. Lu, Y. Liu, *Appl. Catal., B-Environ.* **2012**, *111*, 492.
[111] G. N. Ostojic, M. C. Hersam, *Small* **2012**, *8*, 1840.
[112] X. Zhang, L. Chen, T. Yuan, H. Huang, Z. Sui, R. Du, X. Li, Y. Lu, Q. Li, *Mater. Horiz.* **2014**, *1*, 232.
[113] K. H. Kim, Y. Oh, M. F. Islam, *Nat. Nanotechnol.* **2012**, *7*, 562.
[114] Z. Y. Sui, Q. H. Meng, X. T. Zhang, R. Ma, B. Cao, *J. Mater. Chem.* **2012**, *22*, 8767.
[115] B. You, L. Wang, L. Yao, J. Yang, *Chem. Commun.* **2013**, *49*, 5016.
[116] T. Skaltsas, G. Avgouropoulos, D. Tasis, *Micropor. Mesopor. Mater.* **2011**, *143*, 451.
[117] H. Y. Sun, Z. Xu, C. Gao, *Adv. Mater.* **2013**, *25*, 2554.
[118] M. A. Worsley, J. H. Satcher, T. F. Baumann, *Langmuir* **2008**, *24*, 9763.
[119] M. A. Worsley, S. O. Kucheyev, J. H. Satcher, A. V. Hamza, T. F. Baumann, *Appl. Phys. Lett.* **2009**, *94, 073115*.
[120] M. Wang, I. V. Anoshkin, A. G. Nasibulin, J. T. Korhonen, J. Seitsonen, J. Pere, E. I. Kauppinen, R. H. A. Ras, O. Ikkala, *Adv. Mater.* **2013**, *25*, 2428.
[121] J. G. Duque, C. E. Hamilton, G. Gupta, S. A. Crooker, J. J. Crochet, A. Mohite, H. Htoon, K. A. D. Obrey, A. M. Dattelbaum, S. K. Doorn, *ACS Nano* **2011**, *5*, 6686.
[122] W. Chen, R. B. Rakhi, L. B. Hu, X. Xie, Y. Cui, H. N. Alshareef, *Nano Lett.* **2011**, *11*, 5165.
[123] P. D. Petrov, G. L. Georgiev, *Chem. Commun.* **2011**, *47*, 5768.
[124] W. Chen, R. B. Rakhi, H. N. Alshareef, *J. Mater. Chem.* **2012**, *22*, 14394.
[125] X. Xie, M. Ye, L. B. Hu, N. Liu, J. R. McDonough, W. Chen, H. N. Alshareef, C. S. Criddle, Y. Cui, *Energy Environ. Sci.* **2012**, *5*, 5265.
[126] R. Du, N. Zhang, J. H. Zhu, Y. Wang, C. Y. Xu, Y. Hu, N. N. Mao, H. Xu, W. J. Duan, L. Zhuang, L. T. Qu, Y. L. Hou, J. Zhang, unpublished.

[127] M. C. Gutierrez, M. J. Hortigüela, J. M. Amarilla, R. Jiménez, M. L. Ferrer, F. del Monte, *J. Phys. Chem. C* **2007**, *111*, 5557.
[128] M. C. Gutierrez, M. L. Ferrer, F. del Monte, *Chem. Mater.* **2008**, *20*, 634.
[129] S. M. Kwon, H. S. Kim, H. J. Jin, *Polymer* **2009**, *50*, 2786.
[130] J. Zou, J. Liu, A. S. Karakoti, A. Kumar, D. Joung, Q. Li, S. I. Khondaker, S. Seal, L. Zhai, *ACS Nano* **2010**, *4*, 7293.
[131] T. A. Asoh, A. Kikuchi, *Chem. Commun.* **2012**, *48*, 10019.
[132] Y. L. Zhang, L. Tao, S. X. Li, Y. Wei, *Biomacromolecules* **2011**, *12*, 2894.
[133] Y. Li, J. Chen, L. Huang, C. Li, J. D. Hong, G. Shi, *Adv. Mater.* **2014**, *26*, 4789.
[134] S. Barg, F. M. Perez, N. Ni, P. do Vale Pereira, R. C. Maher, E. Garcia-Tuñon, S. Eslava, S. Agnoli, C. Mattevi, E. Saiz, *Nat. Commun.* **2014**, *5*, 4328.
[135] Y. Tao, X. Y. Xie, W. Lv, D. M. Tang, D. B. Kong, Z. H. Huang, H. Nishihara, T. Ishii, B. H. Li, D. Golberg, F. Y. Kang, T. Kyotani, Q. H. Yang, *Sci. Rep.* **2013**, *3*, 2975.
[136] M. A. Worsley, S. Charnvanichborikarn, E. Montalvo, S. J. Shin, E. D. Tylski, J. P. Lewicki, A. J. Nelson, J. H. Satcher, J. Biener, T. F. Baumann, S. O. Kucheyev, *Adv. Funct. Mater.* **2014**, *24*, 4259.
[137] K. Wepasnick, B. Smith, J. Bitter, D. Howard Fairbrother, *Anal. Bioanal. Chem.* **2010**, *396*, 1003.
[138] Q. Zhao, J. Zhang, *Small* **2014**, *10*, 4586.
[139] D. C. Marcano, D. V. Kosynkin, J. M. Berlin, A. Sinitskii, Z. Z. Sun, A. Slesarev, L. B. Alemany, W. Lu, J. M. Tour, *ACS Nano* **2010**, *4*, 4806.
[140] Y. G. Li, W. Zhou, H. L. Wang, L. M. Xie, Y. Y. Liang, F. Wei, J. C. Idrobo, S. J. Pennycook, H. J. Dai, *Nat. Nanotechnol.* **2012**, *7*, 394.
[141] L. Wang, A. Ambrosi, M. Pumera, *Angew. Chem. Int. Ed.* **2013**, *52*, 13818.
[142] C. L. Pint, Z. Z. Sun, S. Moghazy, Y. Q. Xu, J. M. Tour, R. H. Hauge, *ACS Nano* **2011**, *5*, 6925.
[143] K. Sing, D. Everett, R. Haul, L. Moscou, R. Pierotti, J. Rouquerol, T. Siemieniewska, *Pure Appl. Chem* **1982**, *54*, 2201.
[144] Q. Lu, G. Keskar, R. Ciocan, R. Rao, R. B. Mathur, A. M. Rao, L. L. Larcom, *J. Phys. Chem. B* **2006**, *110*, 24371.
[145] C. Laurent, E. Flahaut, A. Peigney, *Carbon* **2010**, *48*, 2994.
[146] K. J. Zhang, A. Yadav, K. H. Kim, Y. Oh, M. F. Islam, C. Uher, K. P. Pipe, *Adv. Mater.* **2013**, *25*, 2926.
[147] P. W. West, *Rev. Sci. Instrum.* **1999**, *70*, 2802.
[148] Q. Wu, Y. X. Xu, Z. Y. Yao, A. R. Liu, G. Q. Shi, *ACS Nano* **2010**, *4*, 1963.
[149] Y. Zhao, C. Hu, Y. Hu, H. Cheng, G. Shi, L. Qu, *Angew. Chem.* **2012**, *124*, 11533.
[150] R. Kotz, M. Carlen, *Electrochim. Acta* **2000**, *45*, 2483.
[151] M. D. Stoller, R. S. Ruoff, *Energy Environ. Sci.* **2010**, *3*, 1294.
[152] L. L. Zhang, X. S. Zhao, *Chem. Soc. Rev.* **2009**, *38*, 2520.
[153] A. S. Arico, P. Bruce, B. Scrosati, J. M. Tarascon, W. Van Schalkwijk, *Nature Mater.* **2005**, *4*, 366.
[154] K. Katuri, M. L. Ferrer, M. C. Gutierrez, R. Jimenez, F. del Monte, D. Leech, *Energy Environ. Sci.* **2011**, *4*, 4201.
[155] J. Zhang, X. Liu, R. Blume, A. Zhang, R. Schlögl, D. S. Su, *Science* **2008**, *322*, 73.
[156] K. Gong, F. Du, Z. Xia, M. Durstock, L. Dai, *Science* **2009**, *323*, 760.
[157] Z. Chen, D. Higgins, Z. Chen, *Carbon* **2010**, *48*, 3057.
[158] Z. Chen, D. Higgins, Z. Chen, *Electrochim. Acta* **2010**, *55*, 4799.
[159] X. C. Gui, H. B. Li, K. L. Wang, J. Q. Wei, Y. Jia, Z. Li, L. L. Fan, A. Y. Cao, H. W. Zhu, D. H. Wu, *Acta Mater.* **2011**, *59*, 4798.
[160] H. B. Li, X. C. Gui, L. H. Zhang, S. S. Wang, C. Y. Ji, J. Q. Wei, K. L. Wang, H. W. Zhu, D. H. Wu, A. Y. Cao, *Chem. Commun.* **2010**, *46*, 7966.
[161] L. Wang, M. Wang, Z. H. Huang, T. X. Cui, X. C. Gui, F. Y. Kang, K. L. Wang, D. H. Wu, *J. Mater. Chem.* **2011**, *21*, 18295.
[162] Z. Peng, D. S. Zhang, T. T. Yan, J. P. Zhang, L. Y. Shi, *Appl. Surf. Sci.* **2013**, *282*, 965.
[163] H. Bi, Z. Yin, X. Cao, X. Xie, C. Tan, X. Huang, B. Chen, F. Chen, Q. Yang, X. Bu, X. Lu, L. Sun, H. Zhang, *Adv. Mater.* **2013**, *25*, 5916.
[164] L. T. Qu, L. M. Dai, M. Stone, Z. H. Xia, Z. L. Wang, *Science* **2008**, *322*, 238.
[165] X. C. Gui, H. B. Li, L. H. Zhang, Y. Jia, L. Liu, Z. Li, J. Q. Wei, K. L. Wang, H. W. Zhu, Z. K. Tang, D. H. Wu, A. Y. Cao, *ACS Nano* **2011**, *5*, 4276.
[166] F. F. Zhang, J. Tang, Z. H. Wang, L. C. Qin, *Chem. Phys. Lett.* **2013**, *590*, 121.
[167] A. Abarrategi, M. C. Gutierrez, C. Moreno-Vicente, M. J. Hortiguela, V. Ramos, J. L. Lopez-Lacomba, M. L. Ferrer, F. del Monte, *Biomaterials* **2008**, *29*, 94.
[168] A. E. Aliev, J. Oh, M. E. Kozlov, A. A. Kuznetsov, S. Fang, A. F. Fonseca, R. Ovalle, M. D. Lima, M. H. Haque, Y. N. Gartstein, *Science* **2009**, *323*, 1575.
[169] Z. P. Zeng, X. C. Gui, Z. Q. Lin, L. H. Zhang, Y. Jia, A. Y. Cao, Y. Zhu, R. Xiang, T. Z. Wu, Z. K. Tang, *Adv. Mater.* **2013**, *25*, 1185.
[170] M. Motta, Y. L. Li, I. Kinloch, A. Windle, *Nano Lett.* **2005**, *5*, 1529.
[171] Q. Peng, Y. Li, X. He, X. Gui, Y. Shang, C. Wang, C. Wang, W. Zhao, S. Du, E. Shi, *Adv. Mater.* **2014**, *26*, 3241.

Received: October 27, 2014
Revised: December 24, 2014
Published online: March 4, 2015

